THE JOURNAL OF BIOLOGICAL CHEMISTRY VOL. 285, NO. 34, pp. 26390–26405, August 20, 2010
© 2010 by The American Society for Biochemistry and Molecular Biology, Inc. Printed in the U.S.A.

$GABA_A$ Receptor α1 Subunit Mutation A322D Associated with Autosomal Dominant Juvenile Myoclonic Epilepsy Reduces the Expression and Alters the Composition of Wild Type $GABA_A$ Receptors*[S]

Received for publication, May 10, 2010, and in revised form, June 11, 2010 Published, JBC Papers in Press, June 15, 2010, DOI 10.1074/jbc.M110.142299

Li Ding[‡], Hua-Jun Feng[‡], Robert L. Macdonald[‡§¶], Emanuel J. Botzolakis[‡], Ningning Hu[‡], and Martin J. Gallagher[‡1]

From the Departments of [‡]Neurology, [§]Molecular Physiology and Biophysics, and [¶]Pharmacology, Vanderbilt University, Nashville, Tennessee 37232

A $GABA_A$ receptor ($GABA_AR$) α1 subunit mutation, A322D (AD), causes an autosomal dominant form of juvenile myoclonic epilepsy (ADJME). Previous studies demonstrated that the mutation caused α1(AD) subunit misfolding and rapid degradation, reducing its total and surface expression substantially. Here, we determined the effects of the residual α1(AD) subunit expression on wild type $GABA_AR$ expression to determine whether the AD mutation conferred a dominant negative effect. We found that although the α1(AD) subunit did not substitute for wild type α1 subunits on the cell surface, it reduced the surface expression of $\alpha1\beta2\gamma2$ and $\alpha3\beta2\gamma2$ receptors by associating with the wild type subunits within the endoplasmic reticulum and preventing them from trafficking to the cell surface. The α1(AD) subunit reduced surface expression of $\alpha3\beta2\gamma2$ receptors by a greater amount than $\alpha1\beta2\gamma2$ receptors, thus altering cell surface $GABA_AR$ composition. When transfected into cultured cortical neurons, the α1(AD) subunit altered the time course of miniature inhibitory postsynaptic current kinetics and reduced miniature inhibitory postsynaptic current amplitudes. These findings demonstrated that, in addition to causing a heterozygous loss of function of α1(AD) subunits, this epilepsy mutation also elicited a modest dominant negative effect that likely shapes the epilepsy phenotype.

$GABA_ARs$[2] are ligand-gated ion channels that provide the major source of inhibitory control to the mammalian central nervous system. Each $GABA_AR$ is a pentamer whose five subunits arise from seven subunit families that contain multiple subtype isoforms. Neurons preferentially express $GABA_ARs$ composed of distinct combinations of subunit isoforms in different brain regions at well defined times in development (1–3). At maturity, the most prevalent $GABA_AR$ throughout the brain consists of two α1 subunits, two β2 subunits, and one γ2 subunit in a β2-α1-β2-α1-γ2 assembly (4–6). To date, 13 autosomal dominant mutations in $GABA_AR$ subunit genes have been associated with different epilepsy syndromes (7).

The missense AD mutation in the $GABA_AR$ α1 subunit gene (*GABRA1*) causes ADJME (8), a monogenic form of a common epilepsy syndrome that begins at a distinct developmental time point (adolescence) and confers myoclonic, generalized tonic-clonic, and absence seizures as well as neuropsychiatric comorbidities (9). We demonstrated previously that the AD mutation, which substitutes a negatively charged aspartate for a neutral alanine within the M3 transmembrane domain, causes the α1(AD) subunit to misfold with altered topology (10). Cells rapidly degrade the misfolded α1(AD) subunit through both proteasome- and lysosome-mediated processes (10, 11). Therefore, the α1(AD) subunit is expressed at substantially lower levels than the wild type α1 subunit. $GABA_ARs$ that do incorporate the residual, nondegraded α1(AD) subunits exhibit substantially altered electrophysiological properties (8, 12, 13). Therefore, a major consequence of heterozygous expression of the AD mutation is a heterozygous loss of functional α1 subunits.

However, it is unlikely that α1 subunit haploinsufficiency alone explains the entire ADJME phenotype. Heterozygous *Gabra1* knock-out mice do not exhibit spontaneous behavioral seizures. Moreover, a recently discovered *GABRA1* frameshift mutation that causes complete elimination of the mutant α1 subunit protein causes a much milder form of epilepsy than juvenile myoclonic epilepsy (14, 15). These findings suggest that despite being misfolded and substantially degraded, the residual α1(AD) subunit likely has other pathophysiological actions that lead to a more severe phenotype than would be caused by haploinsufficiency alone. Recently, an extremely small dominant negative effect caused by another epilepsy-associated $GABA_AR$ subunit mutation, γ2(R43Q), proved to be critical for causing the epilepsy phenotype (16–19). Therefore, we set out to determine whether the α1(AD) subunit altered wild type $GABA_AR$ expression, physiology, or cellular viability.

MATERIALS AND METHODS

Cell Culture—HEK293T cells were purchased from American Type Culture Collection and were cultured at 37 °C in 5% CO_2, 95% air in Dulbecco's modified Eagle's medium (DMEM,

* This work was supported, in whole or in part, by National Institutes of Health Grants NS055979 (to M. J. G.), NS33300 (to R. L. M.), and NS51590 (to R. L. M.) from the USPHS.

[S] The on-line version of this article (available at http://www.jbc.org) contains supplemental Figs. 1–3.

[1] To whom correspondence should be addressed: Dept. of Neurology, Vanderbilt University, 6140 Medical Research Bldg. III, 465 21st Ave., South, Nashville, TN 37232-8552. Tel.: 615-322-5979; Fax: 615-322-5517; E-mail: Martin.Gallagher@Vanderbilt.edu.

[2] The abbreviations used are: $GABA_AR$, GABA receptor type A; mIPSC, miniature inhibitory postsynaptic current; ER, endoplasmic reticulum; ADJME, autosomal dominant form of juvenile myoclonic epilepsy; DIV, days *in vitro*.

Invitrogen) with 10% fetal bovine serum (FBS, Invitrogen) and 100 IU/ml streptomycin and penicillin (Invitrogen). Cells were replated twice weekly.

We adapted our neuron culture protocol from one described previously (20). Briefly, we dissected cerebral cortices from the brains of embryonic day 18 (E18) Sprague-Dawley rat pups. After trypsin digestion and trituration, we plated 6.7×10^5 neurons in 35-mm dishes on polyornithine-coated coverslips. The neurons were initially cultured in DMEM containing 80 μM glutamine, 8% FBS, and 8% F-12 nutrient mixture (Invitrogen). After 3 days, we added cytosine arabinoside to a final concentration of 1 μM to control glial proliferation (Sigma). On the following day, we exchanged the media with Neurobasal media that contained B27 supplement (Invitrogen). One-half volumes of Neurobasal media were exchanged three times/week.

Expression Vectors and Transfection—The pcDNA3.1 plasmids containing cDNAs that encode human α1, α1(AD), β2S, and γ2S $GABA_AR$ receptor subunits were described previously (10, 13, 21). The DNA encoding the α3 subunit was obtained from Origin Technologies, Inc. It was subcloned into the pcDNA3.1 vector and modified to match the coding sequences found in the GenBank™ and Swiss Protein Databases. The cDNA encoding hemagglutinin (HA) epitope-tagged transforming growth factor α (TGF^{HA}) protein was generously contributed by Dr. Robert Coffey, Vanderbilt University. The pmaxGFP vector was from Lonza. The wild type and dominant negative K44A dynamin1 plasmids were a kind gift from Dr. Pietro De Camilli (Yale University). We purchased the pLVX-IRES-ZsGreen1 bicistronic vector from Clontech.

In this study, we numbered amino acids starting from the initiation methionine in the signal peptide. Using standard molecular biology techniques, we deleted the codon that encodes leucine 31 (leucine 4 as numbered from the putative N terminus of the mature peptide) from the human α1 subunit cDNA ($\alpha1^h$) to make a cDNA encoding the rat α1 subunit ($\alpha1^r$). We also introduced the nucleotides encoding the hemagglutinin (HA) epitope tag (YPYDVPDYA) between the codons encoding the 31st and 32nd amino acids (fourth and fifth amino acids as numbered from the putative N terminus of the mature peptide) of the $\alpha1^h$ subunit to form the $\alpha1^{HA}$ subunit. Similarly, we inserted the HA epitope in the homologous positions of the β2 and γ2 sequences to form the $\beta2^{HA}$ and $\gamma2^{HA}$ subunits. We made the AD mutation in the $\alpha1^{HA}$ and $\alpha1^r$ subunit cDNA using the QuikChange site-directed mutagenesis kit (Stratagene). To make constructs for use in neuronal transfections, we inserted the cDNA encoding the human α1, α1(AD), $\alpha1^{HA}$, and $\alpha1(AD)^{HA}$ subunits into the pLVX-IRES-ZsGreen1 vector.

We transfected HEK293T cells in 6-cm dishes with 3 μg of total cDNA using the FuGENE 6 transfection reagent (Roche Diagnostics, 3 μl/μg DNA). The amount of cDNA encoding each subunit is listed in the figure legends. If the total $GABA_AR$ subunit cDNA was less than 3 μg, we added sufficient empty pcDNA3.1 vector so that the total DNA transfected equaled 3 μg. Neurons were transfected 10 days after plating (DIV10) using a calcium phosphate method as described elsewhere (22).

Antibodies—The mouse monoclonal anti-α1 subunit antibody N95/35 was from the University of California, Davis/National Institutes of Health NeuroMab Facility. The mouse monoclonal anti-human $GABA_AR$ α1 ($\alpha1^h$) subunit antibody (BD24), the rabbit polyclonal anti-rat α1 subunit antibody ($\alpha1^r$, 06-868, lot 026K4848), the rabbit polyclonal anti-β2 subunit antibody (AB5561, lot LV1512412), and the mouse monoclonal anti-neuronal nuclei (NeuN) antibody (clone A60) were from Millipore. The rabbit polyclonal anti-$GABA_AR$ α3 subunit antibody (AGA-003, lot AN-02) was from Alamone. The unconjugated and Alexa 647- (A647) and Alexa 555 (A555)-conjugated mouse monoclonal anti-HA antibodies (HA-555, HA-647) were from Covance (clone 16B12). The rabbit polyclonal anti-glyceraldehyde-3-phosphate dehydrogenase (GAPDH, AB948, lot 708812) and mouse monoclonal anti-sodium potassium ATPase α1 subunit (ATPase, AB7671) were from Abcam. For the flow cytometry experiments, we directly conjugated the mouse anti-$\alpha1^h$ antibody to the A647 fluorphore ($\alpha1^h$-647) using a commercial monoclonal antibody labeling reagent (Invitrogen).

Biotinylation and Western Blot Assays—The biotinylation and Western blot assays have been described previously (13, 23). Briefly, live cells were washed in PBS containing 1 mM $CaCl_2$ and 0.5 mM $MgCl_2$ (PBS-CM) and incubated with the membrane-impermeable, amine-reactive biotinylation reagent, NHS-SS-biotin (3 mM, Thermo), for 15 min at 4 °C. The biotinylation reaction was quenched by washing the cells three times with PBS-CM containing 100 mM glycine.

We lysed the biotinylated cells in modified radioimmunoassay solution (RIPA, 20 mM Tris, pH 7.4, 1% Triton X-100, 250 mM NaCl, 0.5% deoxycholate, 0.1% SDS) that also contained 1 pellet of protease inhibitor per 10 ml (Roche Diagnostics). The lysates were centrifuged at 10,000 $\times$ *g* for 30 min, and the protein concentration was measured using a bicinchoninic acid-based assay (Thermo). To determine total $GABA_AR$ subunit expression, we applied the unpurified lysates directly to a 10% SDS-polyacrylamide gel. To measure surface protein, we incubated equal masses of biotinylated lysates with immobilized neutravidin beads (Thermo) overnight. The neutravidin beads were washed with RIPA buffer, and the biotinylated protein was liberated by incubation with Laemmli sample buffer and fractionated on a 10% SDS-polyacrylamide gel. We confirmed that the proteins of interest did not nonspecifically adhere to the neutravidin beads by also incubating lysates from nonbiotinylated cells with the beads before applying them to SDS-PAGE (data not shown). In each experiment, we confirmed that the biotinylation reagent did not modify intracellular proteins by measuring GAPDH immunoreactivity in the neutravidin-purified lysates (data not shown).

After SDS-PAGE, we electrotransferred the proteins to nitrocellulose membranes. For the Western blots using the anti-α1, -$\alpha1^h$, -α3, -β2, -ATPase, and -GAPDH antibodies, we blocked the membranes with Tris-buffered saline containing 0.1% Tween (TTBS) and 5% nonfat milk. We blocked the Western blots using the anti-HA antibody with PBS containing 0.1% Tween and 0.5% bovine serum albumin (BSA, Sigma).

After incubation with the primary antibody, the immunoblots were incubated with a horseradish peroxidase-coupled goat anti-mouse or anti-rabbit secondary antibody (Jackson ImmunoResearch, 1:5000 dilution) and then visualized with a

chemiluminescent detection system (Amersham Biosciences) using a digital imager (Alpha Innotech). The integrated intensities of the Western blot bands were calculated using the ImageJ software (National Institutes of Health). We confirmed that the integrated intensities of all the bands remained in the linear range of detection by loading three different masses of protein on the gels and performing a linear regression through the origin of the integrated intensity *versus* protein mass. The integrated intensities of all proteins were normalized to the loading control (ATPase).

Flow Cytometry and Fluorescent Resonance Energy Transfer (FRET)—Flow cytometry and FRET were performed as described previously (24, 25). Briefly, transfected cells were detached from the plastic plates by incubating them with trypsin for 1 min at room temperature, a process that does not cause degradation of surface $GABA_AR$ protein (24). All subsequent steps were performed at 0 °C. We stopped the trypsinization by adding 5 ml of FACS buffer (PBS containing 2% FBS and 0.05% sodium azide). The cells were pelleted and placed into 96-well plates. To measure surface protein expression, the cells were stained without fixation, and to measure total protein, the cells were treated with a commercial fixation/permeabilization reagent (BD Biosciences) before staining. The cells were stained with the anti-$\alpha1^h$-647 (1:100), -$\alpha1^r$ (1:50), -$\alpha3$ (1:50), and HA-555 or HA-647 (1:100) antibodies for 1 h. The cells stained with the anti-$\alpha1^r$ and -$\alpha3$ antibodies were then stained with A647-conjugated goat anti-rabbit antibody (1:250, Invitrogen). In each experiment, we confirmed that these dilutions represented saturating concentrations of the respective antibodies by also staining negative control cells and wild type $GABA_AR$ cells with a 2-fold higher concentration of antibody and verifying that the fluorescence did not substantially change (data not shown). After staining, the cells were fixed with 2% paraformaldehyde in PBS.

For each sample, we analyzed 10,000 cells on an LSR II digital flow cytometer (BD Biosciences). We identified viable cells based upon their forward and side scatter properties (data not shown) that were originally determined from staining with the membrane-impermeable dye, 7-aminoactinomycin D (Invitrogen) (24, 25). The A647 fluorophore was excited by a 635 nm laser and detected with a 675/20 bandpass filter, and the A555 fluorophore was excited with a 535 nm laser and detected with a 575/26 bandpass filter. GFP was excited by a 488-nm laser and detected using a 530/30 bandpass filter. In each of the samples, we measured the mean GFP, A555, and A647 fluorescence in viable cells using the FlowJo 7.2 software (Treestar) and subtracted the mean fluorescence obtained from negative control cells.

We measured the FRET between the samples stained with A555-coupled antibody (donor) and a A647-coupled antibody (acceptor) by exciting the A555 fluorophore with the 535-nm laser and detecting the FRET to the A647 fluorophore using 670/20 bandpass filter. To eliminate the fluorescence resulting from direct 535 nm stimulation to the A555 and A647 fluorophores from the FRET signal, we performed spectral compensation using singly stained samples and the FlowJo 7.2 software (Treestar). We then subtracted the mean FRET fluorescence from the samples stained with only the A647 fluorophore from those stained with both the A555 and A647 fluorophores to calculate the specific mean FRET fluorescence.

Confocal Microscopy and Image Analysis—Microscopic analyses were performed using the coverslips on which the neurons were originally plated. On DIV17, 7 days after transfection, we washed the neurons three times in PBS and then fixed them in 4% paraformaldehyde, 4% sucrose in PBS for 15 min at room temperature. We washed the neurons three times with PBS and then incubated them with 0.1% Triton X-100 in PBS for 5 min before washing three more times with PBS. We blocked nonspecific binding by incubating the fixed neurons with 0.5% BSA in PBS for 1 h at room temperature. We stained the neurons with either anti-NeuN (1:200) or anti-$\alpha1^h$ antibody (1:1000) diluted in 0.2% BSA in PBS overnight at 4 °C. The following day, we washed the neurons five times with PBS and then incubated them for 1 h with Alexa 546-conjugated goat anti-mouse antibody diluted in PBS containing 0.2% BSA. We washed them with PBS five more times and counterstained them with 4′,6-diamidino-2-phenylindole (DAPI).

Confocal imaging was performed through the use of the Vanderbilt University Medical Center Cell Imaging Shared Resource. We visualized the neurons with an Olympus FV1000 confocal microscope using a 60×/1.45 numerical aperture plan-apochromat objective. We used the recommended Olympus laser and filter combinations to separately detect DAPI, ZsGreen1, and A546 fluorescence and used singly stained specimens to verify that these fluorophores did not spectrally overlap. We adjusted the pinhole of all channels to obtain 3-μm sections, and we obtained a single section at the level of the nucleus. In each experiment, we adjusted the laser intensity and detector sensitivity to utilize the full linear range of detection, and we used the same settings for all the samples acquired during the experiment. Images were obtained with 12-bit, 1024 × 1024 pixel resolution.

To determine the percentage of cells in the culture that consisted of neurons, we stained the cells with an antibody against NeuN. In three different regions of the slide, we determined the fraction of cells stained with DAPI that were also stained with NeuN. To determine the percentage of neurons transfected, we calculated the fraction of neurons stained with NeuN that also expressed ZsGreen1.

To determine the expression of recombinant $\alpha1^h$ and $\alpha1(AD)^h$ subunits, we visually identified several ZsGreen1-expressing neurons from each culture. We then acquired confocal images of each neuron. We analyzed the images off line using the ImageJ software. We determined the mean fluorescence of a 5-pixel wide line drawn either through the nucleus (for ZsGreen1 fluorescence) or though the soma excluding the nucleus (for $\alpha1^h$ fluorescence). We normalized the fluorescence of each neuron to the mean fluorescence of the neurons transfected with wild type $\alpha1^h$ that were imaged on the same day.

Electrophysiology—We recorded mIPSCs on pyramidal neurons on DIV17, 7 days after transfection. The coverslips that contained the neurons were placed in 35-mm plastic culture dishes and covered with external recording solution that contained the following (in mM): NaCl (142), HEPES (10), KCl (8), $CaCl_2$ (1), glucose (10), and $MgCl_2$ (6), pH 7.4. We

added 1 μM tetrodotoxin, 40 μM D-(−)-2-amino-5-phosphonovaleric acid, 10 μM 6-cyano-7-nitroquinoxaline-2,3-dione, and 1 μM CGP52432 to the external solution to block action potentials and NMDA, AMPA, and $GABA_B$ currents. The intrapipette solution contained the following (in mM): KCl (153), EGTA (5), HEPES (10), $MgCl_2$ (1), and Mg-ATP (2), pH 7.3. Recording electrodes were pulled from borosilicate capillary glass (Fisher) on a micropipette electrode puller (Sutter) and typically had a resistance of ~2 megohms.

We visually identified transfected pyramidally shaped neurons by ZsGreen1 fluorescence using an inverted fluorescence microscope (Nikon). After making a gigaohm seal with the soma, we broke through the membrane to establish electrical contact with the cytoplasm. We voltage-clamped the neurons at −60 mV using an Axopatch 200B amplifier and using the pClamp software (Molecular Devices). We recorded more than 100 mIPSC events from each neuron. Each mIPSC recording was analyzed off line by an investigator who was blinded to the transfection conditions. The mIPSCs were chosen manually using the Mini Analysis software (Synaptosoft). The detection threshold was set at 15 pA. The inter-mIPSC intervals, mIPSC amplitude, rise time, and decay time constants were recorded.

Data Analysis—Expression levels of the $GABA_AR$ subunits were normalized to those obtained from the wild type condition and were reported as means ± S.E. Statistical significance was determined using the Student's paired or unpaired *t* test or paired or unpaired analysis of variance test, as appropriate.

To simplify the presentation of our data, which determined the effects of co-transfecting different masses of α1(AD) subunit cDNA on wild type $GABA_AR$ expression, we fit the expression levels to the sigmoidal concentration-response equation as follows: $Y = 100\%/(1 + (X/IC_{50})^{\text{Hill slope}})$, where *Y* is the expression level of the $GABA_AR$ subunit normalized to that obtained in the absence of the α1(AD) subunit, and *X* is the mass of α1(AD) subunit cDNA. We must emphasize that although we connected our data points with the fit concentration dependence equation, we are not asserting that the α1(AD) subunit necessarily acted by binding competitively with wild type $GABA_ARs$. Therefore, we made statistical comparisons between the mean expression levels instead of the fit IC_{50} and Hill slope values.

The mIPSC inter-mIPSC intervals, rise times, decay time constants, and peak amplitudes were compared using both a nonparametric analysis of variance and Kolmogorov-Smirnov tests. For the Kolmogorov-Smirnov test, the Bonferroni correction was applied to assess statistical significance among the three transfection conditions.

RESULTS

Heterozygous Cells Express Greater Amounts of Total α1 Subunit Protein than Hemizygous Cells—As a first step to determine whether expression of the α1(AD) subunit altered expression of α1β2γ2 receptors, we co-transfected HEK293T cells with 0.250 μg of β2 and γ2 subunit cDNA and either 0.250 μg of α1 subunit (wild type (WT)), 0.125 μg of α1 subunit (hemizygous), 0.125 μg of α1 subunit plus 0.125 μg α1(AD) subunit (heterozygous), or 0.250 μg of α1(AD) subunit (homozygous) cDNA. We use the terms hemizygous, heterozygous, and homozygous solely as a convenient naming convention to convey the ratio of masses of wild type to mutant cDNAs transfected. We used biotinylation assays and Western blots to determine the amount of surface and total α1 subunit expression in each of these transfection conditions (Fig. 1, *A–D*). As described previously, both surface and total heterozygous and homozygous α1 subunit expression differed substantially from each other and from wild type α1 subunit expression. Here, we found that both surface and total hemizygous α1 subunit expression was also substantially reduced compared with wild type expression. However, there was no significant difference between hemizygous and heterozygous α1 subunit expression.

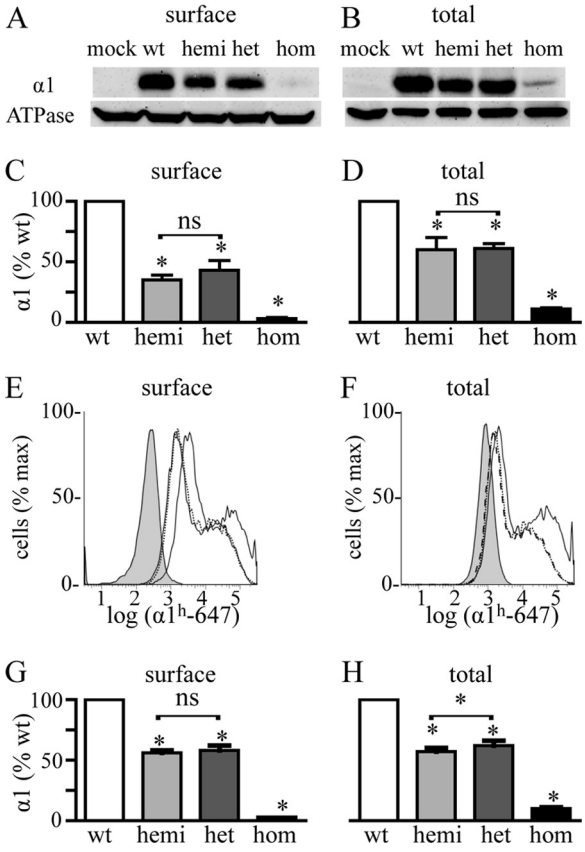

FIGURE 1. **Effect of heterozygous α1(AD) subunit expression on surface and total α1 subunit expression.** We transfected HEK293T cells with empty plasmid (negative control) or 0.250 μg of β2 and γ2 subunit cDNA and either 0.250 μg of wild type α1 (*wt*), 0.125 μg α1 (hemizygous (*hemi*)), 0.125 μg each of α1 and α1(AD) (heterozygous (*het*)), or 0.250 μg of α1(AD) (homozygous (*hom*)) cDNA. We biotinylated surface proteins and performed Western blots to determine the surface (*A* and *C*) and total (*B* and *D*) $GABA_AR$ α1 subunit expression relative to that of the ATPase α1 subunit (loading control). Surface and total hemizygous and heterozygous α1 subunit expression was greater than that of homozygous expression and was significantly reduced relative to wild type expression (*), but there was no significant (*ns*) difference between them ($n = 5$). We also performed flow cytometry assays (*E–H*) as a second method to quantify the surface and total α1 subunit for cells transfected with negative control (*filled histogram*), wild type (*solid line*), hemizygous (*dotted line*), heterozygous (*dashed line*), or homozygous (data not shown) $GABA_AR$. There was no significant difference between hemizygous and heterozygous receptors in surface α1 subunit expression ($n = 7$), but total heterozygous α1 subunit expression was larger than that of hemizygous α1 subunit expression ($n = 6$, $p = 0.03$).

We next used flow cytometry as a second technique to measure surface and total α1 subunit expression (Fig. 1, *E–H*). Previous studies demonstrated that flow cytometry can measure total and surface $GABA_AR$ subunit expression with high preci-

sion and thus could potentially detect differences between hemizygous and heterozygous expression that could not be detected with Western blot assays (24). We found that flow cytometry did quantify α1 subunit expression with smaller standard deviations than Western blot experiments and was able to detect that heterozygous cells expressed 9% more total α1 subunit than hemizygous cells ($p < 0.05$). However, the flow cytometry experiments did not detect a difference between heterozygous and hemizygous cells in surface α1 subunit expression.

Wild Type α1 Subunit Accounted for 92–96% of the Surface α1 Subunit with Heterozygous Expression—The experiments in Fig. 1 demonstrated that compared with hemizygous cells, heterozygous cells possessed increased amounts of total α1 subunit protein but did not have significantly different amounts of surface α1 subunit protein. We thought that the increase in total α1 subunit protein expression in the heterozygous cells likely resulted from the residual, nondegraded α1(AD) subunit in intracellular compartments and that the lack of a significant change in surface expression resulted because the residual α1(AD) subunit did not efficiently traffic to the cell surface. Therefore, we next determined the fraction of surface α1 subunit with heterozygous expression that consisted of wild type or mutant α1 subunit.

Previously, we used α1 and α1(AD) subunits fused to different fluorescent proteins and estimated that 5–25% of surface α1 subunit with heterozygous expression consisted of the α1(AD) subunit (21). Here, we used flow cytometry with two naturally occurring α1 subunits to obtain a more precise estimate of the amount of wild type and mutant α1 subunit on the cell surface in heterozygous expression. Although fluorescent protein- and epitope-tagged $GABA_AR$ subunits incorporate into pentamers to form functional receptors, the addition of the fused fluorescent protein or epitope tag alters post-translational processing and surface expression of the $GABA_AR$ subunits (10, 21). Therefore, we differentiated between wild type and mutant α1 subunits by transfecting cells using natural α1 and α1(AD) subunits from two different species (human and rat) and then detecting them individually with species-selective antibodies. The mature human α1 ($\alpha1^h$) and rat α1 ($\alpha1^r$) subunit proteins differ by only one amino acid; human α1 subunits possess an additional leucine at position 31 (position 4 as numbered from the putative N terminus of the mature peptide) that is absent in the rat sequence (Fig. 2*A*). Two commercially available antibodies, mouse anti-$\alpha1^h$ and rabbit anti-$\alpha1^r$, bind specifically to their respective subunits.

Initial flow cytometry experiments demonstrated that the species-selective antibodies were very specific for the corresponding species of α1 subunit (supplemental Fig. 1). Moreover, the anti-$\alpha1^h$-647 antibody demonstrated remarkable species specificity such that compared with cells transfected with 0.250 μg of β2 and γ2 subunits and only 0.125 μg of the $\alpha1^h$ subunit, cells transfected with a 16-fold excess (2 μg) of $\alpha1^r$ subunit exhibited 0 ± 0% the surface fluorescence and 2 ± 0.2% of the total fluorescence (data not shown). Because the anti-$\alpha1^r$ antibody could not be directly coupled to a fluorophore, its detection required use of a fluorescent secondary antibody, which produced high levels of background staining in permeabilized cells. Therefore, the anti-$\alpha1^r$ antibody was only used for surface staining.

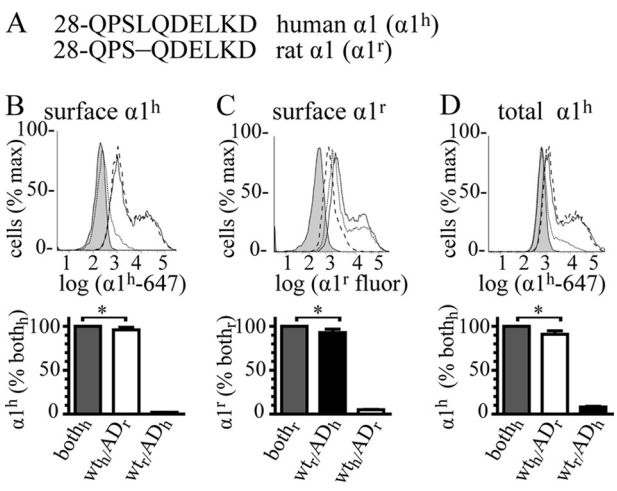

FIGURE 2. **Fraction of wild type α1 and mutant α1(AD) subunits in heterozygous expression.** We depicted the N-terminal amino acids of the mature human ($\alpha1^h$) and rat ($\alpha1^r$) α1 subunits (*A*) with the amino acids numbered starting at the N termini of the signal peptides. The Gln-28 residues are located at the putative N termini of the mature peptides. The full-length mature $\alpha1^h$ and $\alpha1^r$ sequences are identical except that the rat sequence lacks leucine 31 (leucine 4 as numbered from the putative N terminus of the mature peptide). We transfected HEK293T cells with mock vector (negative control, *filled histograms*) or β2 and γ2 subunits (0.250 μg) and heterozygous α1 subunits in which the sequences of the wild type and mutant subunits were both human or both rat (*both$_h$*, *both$_r$*, *solid lines* and *gray bars*). We also transfected cells with heterozygous receptors in which the sequence of the wild type subunit was human and the mutant subunit was rat (*wt$_h$/AD$_r$*, *dashed lines, white bars*), and the sequence of the wild type subunit was rat and the mutant subunit was human (*wt$_r$/AD$_h$*, *dotted lines, black bars*). We stained surface receptors with either the anti-$\alpha1^h$ (*B*) or $\alpha1^r$ antibody (*C*) and total receptors with the anti-$\alpha1^h$ antibody (*D*). We determined the fraction of surface heterozygous subunits composed of wild type subunit by dividing $\alpha1^h$ mean fluorescence in WT^h/AD^r, by the $\alpha1^h$ mean fluorescence in both$_h$ cells (*B*, 96 ± 3%). We obtained a similar result when we divided $\alpha1^r$ staining in WT^r/AD^h cells by that in both$_r$ cells (*C*, 92 ± 2%). Similarly, we determined the fraction of mutant subunit in surface heterozygous receptors by dividing $\alpha1(AD)^h$ staining in WT^r/AD^h cells by that in both$_h$ cells (*B*, 2 ± 0.1%) and dividing $\alpha1(AD)^r$ staining in WT^h/AD^r cells by both$_r$ cells (*C*, 5 ± 0.4%). In total, heterozygous subunits, the wild type $\alpha1^h$ subunit included 91 ± 4% heterozygous expression and the mutant $\alpha1^h$ subunit included 8 ± 4% heterozygous expression. In both surface and total heterozygous expression, the contribution of the wild type subunit was modestly but significantly (*, $p < 0.05$) less than 100%.

We transfected HEK293T cells with 0.250 μg of β2 and γ2 subunit cDNA and heterozygous α1 subunit consisting of either 0.125 μg of cDNA each of $\alpha1^h$ and $\alpha1(AD)^h$ subunits (both human, both$_h$), $\alpha1^r$ and $\alpha1(AD)^r$ subunits (both rat, both$_r$), $\alpha1^h$ and $\alpha1(AD)^r$ subunits (WT_h/AD_r), or $\alpha1^r$ and $\alpha1(AD)^h$ subunits (WT_r/AD_h). We stained surface protein with the anti-$\alpha1^h$ subunit antibody, quantified the fluorescence with flow cytometry, and divided the WT_h/AD_r and WT_r/AD_h fluorescence by that obtained from cells transfected with both human. These data demonstrated that with heterozygous expression, wild type $\alpha1^h$ subunits and mutant $\alpha1(AD)^h$ subunits included 96 ± 3 and 2 ± 0.1% of the surface α1 subunit expression, respectively (Fig. 2*B*). These results were concordant with the complementary experiment in which we stained surface protein with the anti-$\alpha1^r$ antibody and found that the wild type $\alpha1^r$ subunits and mutant $\alpha1(AD)^r$ subunits included 92 ± 2 and 5 ± 0.4% of the surface α1 subunit expression (Fig. 2*C*). In permeabilized cells, wild type $\alpha1^h$ subunits and mutant

$\alpha1(AD)^h$ subunits included 91 ± 4 and 8 ± 4% of total $\alpha1$ subunit (Fig. 2*D*). Therefore, the preponderance (92–96%) of $\alpha1$ subunits on the surface of heterozygous cells was wild type $\alpha1$ subunits.

Our data also demonstrated that in both surface and total heterozygous expression, the contribution of the wild type subunit was modestly, but significantly ($p < 0.05$), less than 100%. This result suggests that the mutant $\alpha1(AD)$ subunit could cause a dominant negative effect either by substituting for wild type $\alpha1$ subunit or by reducing wild type $\alpha1$ subunit surface expression.

Finally, we compared the surface expression of wild type $\alpha1^h$ or $\alpha1^r$ protein in heterozygous cells (WT_h/AD_r or WT_r/AD_h) with the corresponding hemizygous receptors (hemizygous $\alpha1^h$ or $\alpha1^r$). The presence of the mutant subunit caused small but, in the case of the $\alpha1^r$ protein, statistically significant reductions in surface wild type $\alpha1$ subunit protein expression (8 ± 2%, $p = 0.009$, not shown). This result also suggested that the $\alpha1(AD)$ subunit could reduce wild type $\alpha1$ subunit surface expression.

α1(AD) Subunit Did Not Substitute for Wild Type α1 Subunits on the Cell Surface—Experiments in Fig. 2 demonstrated that when heterozygously expressed in HEK293T cells, mutant $\alpha1(AD)$ subunits included 8% of the total $\alpha1$ subunits and 2–5% of the surface $\alpha1$ subunits. However, the fraction of mutant $\alpha1(AD)$ subunits expressed in neurons from ADJME patients is unknown. If the neurons of patients expressed a greater fraction of total $\alpha1(AD)$ subunit than HEK293T cells, would more $\alpha1(AD)$ subunit be expressed on the cell surface and confer a dominant negative effect by substituting mutant $\alpha1(AD)$ subunits for wild type $\alpha1$ subunits?

In a heterologous expression system, we can increase the amount of protein expression by increasing the mass of cDNA transfected. Therefore, we transfected cells with $\beta2$ and $\gamma2$ subunit cDNA (0.250 μg) and hemizygous (0.125 μg) $\alpha1^r$ subunits and a range (0- 2 μg) of wild type $\alpha1^h$ or $\alpha1(AD)^h$ $\alpha1$ cDNA. We quantified the amount of relative total and surface $\alpha1^h$ and $\alpha1(AD)^h$ subunit expression by flow cytometry and normalized all the values to the total or surface expression cells transfected with hemizygous $\alpha1^h$ ("positive control," $\alpha1^h\beta2\gamma2$ 0.125, 0.250, and 0.250 μg).

As expected, increasing the masses of wild type $\alpha1^h$ and $\alpha1(AD)^h$ subunit cDNA increased the amount of total $\alpha1^h$ and $\alpha1(AD)^h$ subunit expression (Fig. 3, *A* and *C*). The total $\alpha1(AD)^h$ subunit expression increased linearly with the mass of cDNA from 0 to 2 μg, and the total $\alpha1^h$ subunit expression increased linearly from 0 to 0.5 μg of cDNA before saturating. Because the $\alpha1(AD)$ subunit was degraded, total $\alpha1(AD)^h$ subunit expression was smaller than total $\alpha1^h$ subunit expression.

Increasing the mass of $\alpha1^h$ subunit cDNA increased the amount of surface $\alpha1^h$ subunit expression. In contrast, increasing the mass of $\alpha1(AD)^h$ subunit cDNA caused little change in surface $\alpha1(AD)^h$ expression (Fig. 3, *B* and *D*). Replotting the surface $\alpha1^h$ and $\alpha1(AD)^h$ expression *versus* total $\alpha1^h$ and $\alpha1(AD)^h$ expression (Fig. 3*E*) demonstrated that at the same amount of total $\alpha1^h$ and $\alpha1(AD)^h$ subunit expression there was 8-fold more $\alpha1^h$ subunit on the cell surface. Repeating these studies using cells lacking the hemizygous $\alpha1^r$ subunit produced identical results (data not shown). These data demonstrated that in addition to reducing total $\alpha1(AD)$ expression, the AD mutation also strongly inhibited the surface expression of receptors containing the $\alpha1(AD)$ subunit. Therefore, even if neurons from ADJME patients expressed larger relative amounts of $\alpha1(AD)$ subunits than HEK293T cells, the mutant subunits would not produce a dominant negative effect by substituting for wild type subunits on the cell surface.

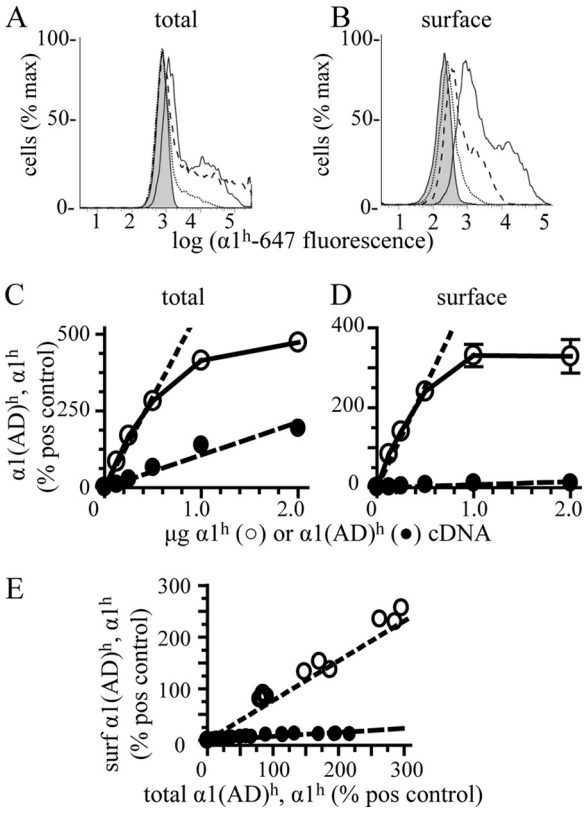

FIGURE 3. **Effect of increasing mutant α1(AD) subunit cDNA on surface and total α1(AD) subunit protein expression.** We transfected HEK293T cells with empty vector (negative control, *shaded histograms*) or 0.250 μg of $\beta2$ and $\gamma2S$ subunits and 0.125 μg of $\alpha1^h$ subunit cDNA (hemizygous positive control, *solid line histogram*) or 0.250 μg of $\beta2$ and $\gamma2S$ subunits, 0.125 μg of $\alpha1^r$ subunit, and increasing amounts of either $\alpha1(AD)^h$ or $\alpha1^h$ subunit cDNA. We measured the total (*A* and *C*) and surface (*B* and *D*) $\alpha1(AD)^h$ and $\alpha1^h$ subunit fluorescence by flow cytometry. *A* and *B*, *dotted lines* depict the fluorescence of cells transfected with 0.125 μg of $\alpha1(AD)^h$ subunits, and the *dashed lines* depict the fluorescence of cells transfected with 2 μg of $\alpha1(AD)^h$ subunits. *C* and *D*, we depicted the $\alpha1(AD)^h$ (●) and $\alpha1^h$ (○) fluorescence normalized to positive control for each mass of $\alpha1(AD)^h$ or $\alpha1^h$ subunit cDNA that we transfected. When measuring total $\alpha1(AD)^h$ and $\alpha1^h$ expression (*C*), increasing both $\alpha1(AD)^h$ and $\alpha1^h$ subunit cDNA caused linear increases in $\alpha1(AD)^h$ and $\alpha1^h$ subunit protein expression until $\alpha1^h$ subunit expression saturated when it was greater than 300% that of positive (*pos*) control. When measuring surface $\alpha1(AD)^h$ and $\alpha1^h$ expression (*D*), increasing $\alpha1^h$ subunit cDNA caused proportional increases in $\alpha1^h$ subunit expression, but increasing $\alpha1(AD)^h$ subunit cDNA resulted in very little change in surface $\alpha1(AD)^h$ subunit expression. *E*, we replotted the surface (*surf*) $\alpha1(AD)^h$ and $\alpha1^h$ subunit expression as a function of total expression. Both surface $\alpha1(AD)^h$ and $\alpha1^h$ subunit expression increased linearly with total expression ($r^2 = 0.82$ and 0.95, respectively, $n \geq 3$). However, there was an 8-fold greater increased surface $\alpha1^h$ subunit expression than $\alpha1(AD)^h$ subunit expression for equal increases in total expression. To determine whether the presence of the wild type $\alpha1^r$ subunit facilitated the surface trafficking of $\alpha1(AD)^h$ subunits, we repeated experiments in the absence of the $\alpha1^r$ subunit and found no significant difference in the surface expression of the $\alpha1(AD)^h$ subunit in the absence of the $\alpha1^r$ subunit ($n = 3$, data not shown).

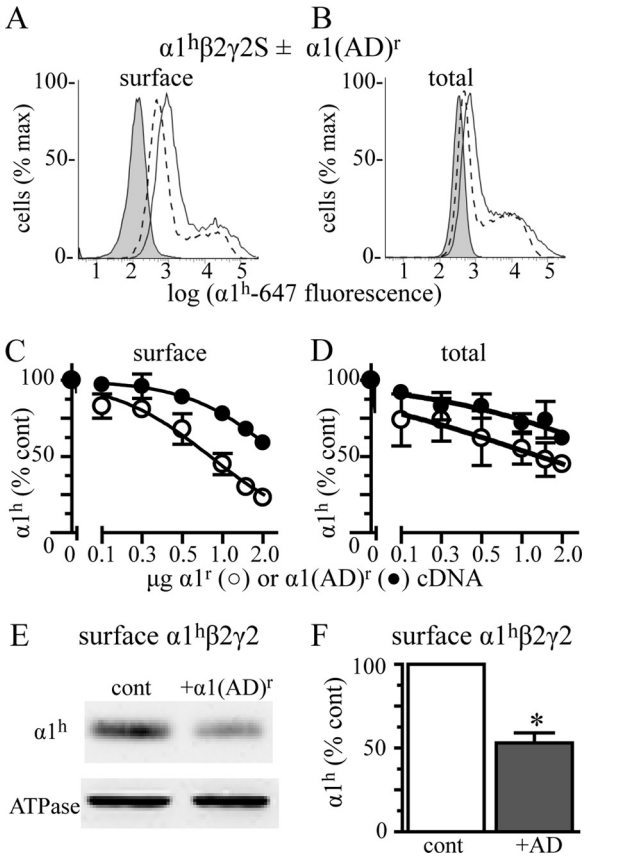

FIGURE 4. **Effect of α1(AD) subunit expression on surface and total α1β2γ2 expression.** We transfected HEK293T cells with empty vector (negative control, *shaded histograms*) or 0.250 μg of β2 and γ2S subunits and 0.125 μg $\alpha1^h$ subunit cDNA (hemizygous) and with varying masses (0–2 μg) of $\alpha1^r$ or $\alpha1(AD)^r$ cDNA. We quantified the surface (*A* and *C*) and total (*B* and *D*) $\alpha1^h$ subunit expression using flow cytometry with anti-$\alpha1^h$ subunit antibodies. *A* and *B*, we depicted hemizygous fluorescence as a *solid line* and hemizygous + 2 μg of $\alpha1(AD)^r$ fluorescence as a *dashed line*. *C* and *D*, we plotted $\alpha1(AD)^h$ (●) and $\alpha1^h$ (○) subunit fluorescence normalized to that of hemizygous subunit fluorescence *versus* the masses of $\alpha1(AD)^h$ or $\alpha1^h$ cDNA that was transfected. Increasing the masses of $\alpha1(AD)^r$ subunit cDNA reduced surface and total $\alpha1^h$ subunit expression. We also determined the effect 2 μg of $\alpha1(AD)^r$ subunit cDNA co-transfection on surface $\alpha1^h\beta2\gamma2$ receptor expression using biotinylation assays with Western blot (*E* and *F*). We stained the Western blots with the anti-$\alpha1^h$ subunit antibody and quantified surface $\alpha1^h$ subunit relative to that of the Na^+/K^+-ATPase α subunit (loading control (*cont*)). The addition of 2 μg of $\alpha1(AD)^r$ subunit cDNA (+*AD*) reduced surface expression of $\alpha1^h\beta2\gamma2$ receptors by 46 ± 6% ($n = 4$; $p = 0.005$). The $\alpha1(AD)^r$ subunit did not alter the surface expression of the endogenous ATPase α subunit (97 ± 10%, $n = 5$).

α1(AD) Subunit Reduced Surface Expression of the Wild Type α1 Subunit—Experiments in Fig. 3 demonstrated that α1(AD) subunits did not cause a dominant negative effect by substituting for wild type α1 subunits on the cell surface, and experiments in Fig. 2 suggested that compared with hemizygous expression the heterozygous expression reduced the wild type α1 subunit on the cell surface. Therefore, we next determined the effect transfecting different amounts of $\alpha1(AD)^r$ subunit on wild type $\alpha1^h$ subunit expression.

We transfected HEK293T cells with β2 and γ2 subunits (0.250 μg), hemizygous (0.125 μg) human $\alpha1^h$ subunits, and a range (0–2 μg) of rat $\alpha1(AD)^r$ cDNAs and measured surface and total $\alpha1^h$ expression by flow cytometry using the anti-$\alpha1^h$ subunit antibody (Fig. 4). For comparison, we also determined the effect of wild type $\alpha1^r$ subunit on $\alpha1^h\beta2\gamma2$ expression. Because the wild type $\alpha1^r$ subunits are not detected by the $\alpha1^h$ subunit antibody, they reduce $\alpha1^h$ subunit expression by substitution rather than $\alpha1(AD)^r$ subunit-mediated inhibition of expression.

The $\alpha1(AD)^r$ subunit caused a concentration-dependent reduction in surface and total $\alpha1^h$ expression (Fig. 4, *A–D*). As expected, the $\alpha1(AD)^r$ subunit caused smaller reductions in $\alpha1^h$ subunit expression than the wild type $\alpha1^r$ subunit. Nonetheless, the $\alpha1(AD)^r$-mediated reduction of $\alpha1^h$ subunit expression demonstrated that nondegraded α1(AD) subunit was not inert and caused a small but potentially clinically significant dominant negative effect by reducing wild type α1 subunit expression.

To confirm that transfection of the $\alpha1(AD)^r$ subunit did not reduce $\alpha1^h\beta2\gamma2$ receptor expression simply by inhibiting the transcriptional or translational capacity of the cells, we compared the effects of transfecting 2 μg of $\alpha1(AD)^r$ or pmaxGFP on $\alpha1\beta2\gamma2$ expression. Cells transfected with pmaxGFP demonstrated strong GFP fluorescence (data not shown). However, unlike the $\alpha1(AD)^r$ subunit, pmaxGFP did not alter surface or total $\alpha1\beta2\gamma2$ receptor expression (supplemental Fig. 2, *A* and *B*).

We used biotinylation assays with Western blotting as a second method to determine the effect of the α1(AD) subunit on surface wild type $\alpha1^h$ subunit expression. We transfected HEK293T cells with β2 and γ2 subunits (0.250 μg) and hemizygous $\alpha1^h$ subunits with or without 2 μg of $\alpha1(AD)^r$ subunit cDNA. We performed biotinylation assays with Western blots and detected the $\alpha1^h$ subunit with the anti-$\alpha1^h$ subunit antibody. Similar to the flow cytometry studies, we found that the $\alpha1(AD)^r$ subunit reduced the surface expression of the wild type $\alpha1^h$ subunit (Fig. 4, *E* and *F*).

Because the α1(AD) subunit is grossly misfolded, it could potentially be a toxic protein and reduce $\alpha1\beta2\gamma2$ expression by nonspecifically decreasing cellular viability. During flow cytometry analyses, we gated viable cells based on their forward and side scatter properties that corresponded to the population of viable cells that excluded the membrane-impermeable dye, 7-aminoactinomycin D (24). We found that transfection of 2 μg of α1(AD) subunit cDNA did not alter the percentage of "viable cells" (62 ± 3%) when compared with cells transfected in the absence of the α1(AD) subunit (60 ± 3%, $n = 5$, $p = 0.710$; data not shown).

To determine whether the α1(AD) subunit inhibited surface expression of $\alpha1\beta2\gamma2$ receptors by nonspecifically preventing surface trafficking of proteins processed through the secretory pathway, we measured the effect of the α1(AD) subunit on the surface expression of two membrane proteins not thought to interact with $GABA_A$Rs. Using biotinylation assays and Western blots, we found that transfection of 2 μg of α1(AD) subunit did not alter the surface expression of the endogenous HEK293T cell Na^+/K^+-ATPase α1 subunit (Fig. 4*E*; 97 ± 10%, $n = 5$, $p = 0.776$). Next, we determined the effect of the $\alpha1(AD)^r$ subunit on surface expression of recombinantly expressed TGF^{HA} protein. We transfected cells with $\alpha1\beta2\gamma2$ receptors, TGF^{HA}, and with or without 2 μg of $\alpha1(AD)^r$ cDNA. We quantified expression of TGF^{HA} by flow cytometry with the anti-HA-647 antibody and found that the α1(AD) subunit did

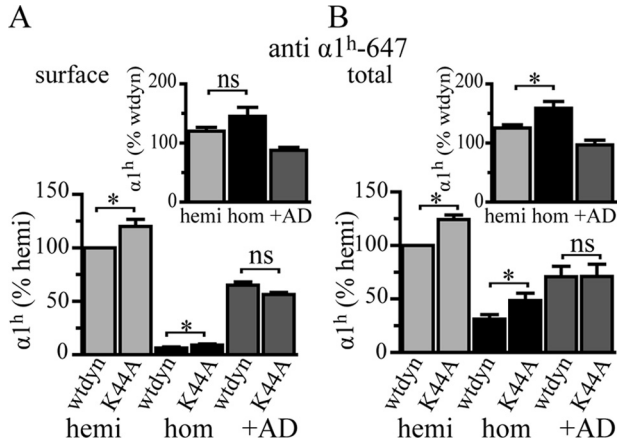

FIGURE 5. **Inhibiting dynamin-mediated endocytosis on the dominant effect of the α1(AD) subunit.** We transfected HEK293T cells with 0.250 μg of β2 and γ2S subunit cDNA and either 0.125 μg of human wild type $\alpha1^h$ subunit (*hemi*, *light gray*), 0.250 μg of human $\alpha1(AD)^h$ subunit (*hom*, *black*), or 0.125 μg of human wild type $\alpha1^h$ subunit and 2 μg $\alpha1(AD)^r$ subunit (+*AD*, *dark gray*). In addition, we also co-transfected the cells with either 0.375 μg of wild type (*wtdyn*) or dominant negative (K44A) dynamin. We measured surface and total human α1 subunit expression by flow cytometry and normalized each value to the expression of the hemizygous samples that were co-transfected with wild type dynamin. In the *insets*, we plotted the percentage change in $\alpha1^h$ and $\alpha1(AD)^h$ expression because of the K44A dynamin. The K44A dynamin increased the total and surface α1 subunit expression in the hemizygous and homozygous conditions ($p < 0.05$), but not alter the dominant effect in the $+\alpha1(AD)^r$ condition ($n = 5$). The K44A dynamin significantly increased total homozygous $\alpha1(AD)^h$ expression to a greater extent than hemizygous $\alpha1^h$ expression ($p < 0.01$). *ns* = $p \geq 0.05$; *, $p < 0.05$.

not reduce expression of TGF^{HA} (116 ± 10%, see supplemental Fig. 3). These data demonstrated that the dominant negative effect conferred by α1(AD) subunit did not result simply by nonspecifically inhibiting protein expression through the secretory pathway.

α1(AD) Subunit Reduced α1 Subunit Expression in a Dynamin-independent Manner—Bradley *et al.* (11) demonstrated that total homozygous $\alpha1(AD)\beta2\gamma2$ expression increased by co-expression of dominant negative dynamin a mutant protein that inhibits clathrin-mediated endocytosis. These data suggested that in addition to causing degradation of the α1(AD) subunit by ER-associated degradation, the AD mutation also increased endocytosis of $\alpha1(AD)\beta2\gamma2$ receptors from the cell surface.

Here, we determined whether the α1(AD) subunit conferred its dominant negative effect by increasing $\alpha1\beta2\gamma2$ receptor endocytosis through a dynamin-dependent mechanism. We co-transfected HEK293T cells with β2 and γ2 subunits and either hemizygous $\alpha1^h$, homozygous $\alpha1(AD)^h$, or hemizygous $\alpha1^h$ subunits that also contained 2 μg of $\alpha1(AD)^r$ cDNA (+AD). In addition, we co-transfected cells with 0.375 μg of cDNA expressing either wild type dynamin or a dominant negative mutant dynamin (K44A) that inhibits endocytosis.

We measured the amount of surface and total human $\alpha1^h$ or $\alpha1(AD)^h$ subunit expression by flow cytometry. In agreement with Bradley *et al.* (11), we demonstrated that co-expression of K44A dynamin increased expression of total homozygous $GABA_A$Rs to a greater extent than "hemizygous" $GABA_A$Rs (Fig. 5*B*). In addition, we demonstrated that K44A dynamin increased surface expression of homozygous receptors to a greater extent than that of hemizygous receptors, although this latter result was not statistically significant (Fig. 5*A*). Although the K44A dynamin did cause a greater effect on homozygous than hemizygous expression, the magnitude of the expression of homozygous receptors was still very small, and thus we do not think that enhanced endocytosis of homozygous $\alpha1(AD)\beta2\gamma2$ makes an appreciable contribution to ADJME pathology. More importantly for the goals of this study, K44A dynamin did not increase the total or surface expression of wild type $\alpha1^h$ subunits when it was co-expressed with $\alpha1(AD)^r$ subunits, and thus the mutant α1(AD) subunit did not produce the dominant negative effect by augmenting dynamin-mediated endocytosis. Interestingly, not only did the K44A dynamin fail to increase expression of the $+\alpha1(AD)^r$ subunit samples to a greater extent than the hemizygous subunit samples, it did not cause *any* increase in $\alpha1^h$ subunit expression, suggesting that the α1(AD) subunit may actually *inhibit* dynamin-mediated endocytosis.

α1(AD) Subunit Associated with Wild Type $GABA_A$R Subunits—Experiments in Fig. 5 demonstrated that the α1(AD) subunit did not confer its dominant negative effect by increasing dynamin-mediated $GABA_A$R endocytosis. Previous studies demonstrated that nondegraded α1(AD) subunits were retained in the ER (21, 26). Could the α1(AD) subunit confer its dominant negative effect by associating with wild type $GABA_A$R subunits and entrapping them in the endoplasmic reticulum (ER)? Bradley *et al.* (11) reported that FLAG epitope-tagged α1(AD) subunits co-immunoprecipitated with γ2-GFP subunit fusion proteins and thus demonstrated that the mutant α1(AD) protein could associate with and potentially entrap wild type $GABA_A$R subunits (11). We extended these studies and used FRET to determine whether α1(AD) subunits specifically associated with wild type $GABA_A$Rs. FRET measures the nonradiative transfer of energy between two fluorophores that are situated within at least 10 nm of one another and can be performed *in situ* in cells using flow cytometry (25, 27).

We transfected HEK293T cells with $\alpha1^{HA}\ \beta2\gamma2$ (Fig. 6*A*), $\alpha1^r\beta2^{HA}\gamma2$ (Fig. 6*B*), or $\alpha1^r\beta2\gamma2^{HA}$ (Fig. 6*C*) receptors. In addition, we co-transfected cells with $\alpha1^r\beta2\gamma2$ receptors and TGF^{HA} protein (Fig. 6*D*). Staining the HA-tagged protein with an A555-conjugated antibody served as the FRET donor. In each of the conditions, we also co-transfected 2 μg of $\alpha1(AD)^h$ subunits that we stained with the A647-conjugated anti-$\alpha1^h$ antibody to serve as the FRET acceptor.

To determine whether or not there were FRET interactions between $\alpha1(AD)^h$ subunits and wild type $GABA_A$R subunits or TGF^{HA} proteins, we excited the FRET donor near its absorption maximum and detected the emission from the FRET acceptor at its emission maximum. In Fig. 6, *A–D*, we plotted flow cytometry histograms that depict the intensity of emission in the FRET channel on the abscissa and the number of cells having that intensity on the ordinate. The *gray plots* in Fig. 6, *A–D*, depict the data for cells stained with only the FRET acceptor and demonstrate the lack of nonspecific FRET signal when the donor was not present. Similar experiments demonstrated even smaller nonspecific FRET signals when the donor but not the acceptor was present (data not shown). The *black plots* in Fig. 6, *A–D*, depict the data for cells stained with both the FRET acceptor and donor. FRET signals are specific when there is

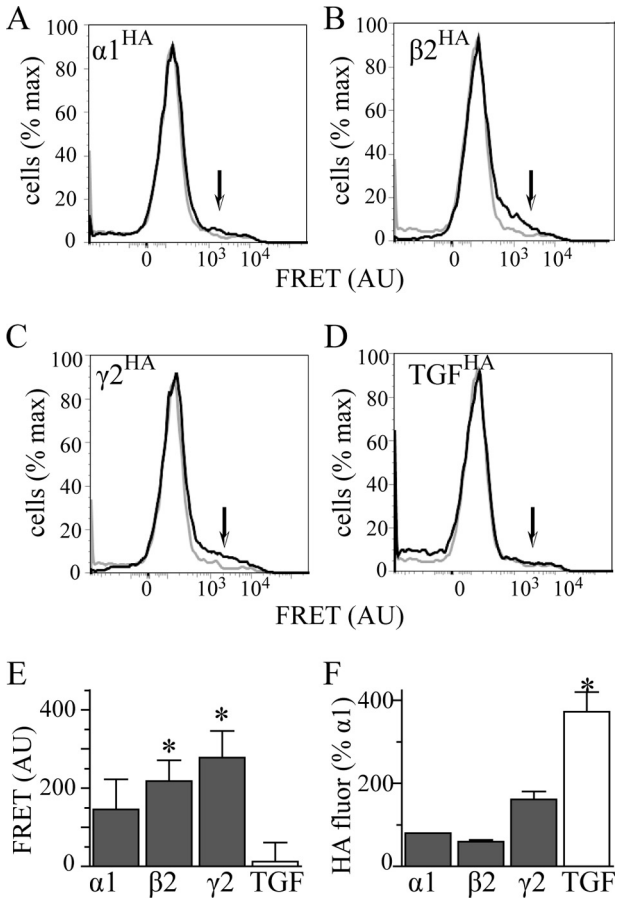

FIGURE 6. **Interactions of the α1(AD) subunit with wild type $GABA_AR$ subunits.** We transfected HEK293T cells with 2 μg of $\alpha1(AD)^h$ subunit and 0.125:0.250:0.250 μg ratios of either $\alpha1^{HA}\beta2\gamma2$ (*A*), $\alpha1^r\beta2^{HA}\gamma2$ (*B*), or $\alpha1^r\beta2\gamma2^{HA}$ subunits to form receptors in which either the α1, β2, or γ2 subunit is tagged with the HA epitope. In addition, to determine whether the $\alpha1(AD)^h$ subunit interacted nonspecifically with the TGF^{HA} protein, we transfected cells with 2 μg of $\alpha1(AD)^h$ subunit, a 0.125:0.250:0.250 μg ratio of $\alpha1^r\beta2\gamma2$ subunits, and 0.250 μg of TGF^{HA} (*D*). We permeabilized the cells and stained them with either the anti-$\alpha1^h$-647 antibody (FRET acceptor), the anti^{HA}-555 antibody (FRET donor), or both anti-$\alpha1^h$-647 and anti^{HA}-555 antibodies. *A–D* are flow cytometry histograms of FRET fluorescence. The *gray line* plots the histogram for cells stained with only the $\alpha1^h$-647 acceptor antibody, and the *black line* plots the histogram for cells stained with both HA-555 donor and $\alpha1^h$-647 acceptor antibodies. The *arrows* point to the regions of the histograms where one would find specific FRET fluorescence. We quantified the specific FRET fluorescence and plotted it in *E* ($n \geq 5$). Samples transfected with $\alpha1\beta2^{HA}\gamma2$ and $\alpha1\beta2\gamma2^{HA}$ receptors possessed substantial FRET fluorescence that significantly differed compared with samples transfected with TGF^{HA} protein. This difference in FRET fluorescence did not result from reduced HA fluorescence from the TGF^{HA} protein because TGF^{HA} possessed substantially more HA florescence than HA-tagged $GABA_AR$ subunits (*F*). AU, arbitrary units.

greater FRET signal in the doubly stained (Fig. 6, *A–D*, *black*) than in the singly stained (*gray*) samples. The regions of the histograms where one finds specific FRET signals are indicated by *arrows* in Fig. 6, *A–D*.

We quantified the specific FRET signals as the difference between the mean FRET emissions of the doubly and singly stained samples. Specific FRET data are summarized in Fig. 6*E* ($n \geq 5$). Both $\beta2^{HA}$ and $\gamma2^{HA}$ subunits, but not the negative control protein TGF^{HA}, demonstrated specific FRET with $\alpha1(AD)^h$ subunits. Although the $\alpha1^{HA}$ also appeared to demonstrate a specific FRET interaction with $\alpha1(AD)^h$, this value was not statistically significant ($p = 0.128$). The lack of FRET interactions between $\alpha1(AD)^h$ subunits and TGF^{HA} protein did not result from decreased donor fluorescence. As demonstrated in Fig. 6*F*, detection of TGF^{HA} protein had substantially *greater* HA-555 florescence than that of the $GABA_AR$ subunits.

These results demonstrated that the α1(AD) subunit specifically associated with other $GABA_AR$ subunits. Based on the prior subcellular localization studies (21, 26), this association must occur in the ER. Because $GABA_ARs$ containing α1(AD) subunits are strongly inhibited from trafficking to the cell surface (Fig. 3), this result suggests that the α1(AD) subunit reduced $GABA_AR$ surface expression by associating with and entrapping $GABA_AR$ in the ER.

α1(AD) Subunit Reduced Surface Expression of α3 Subunit-containing $GABA_ARs$—Neurons predominantly express α2 and α3 subunits early in development and then express α1 subunits later in development. Adult homozygous *Gabra1* knock-out mice express increased amounts of α3 subunits, which partially compensate for the lack of α1 subunits (28–31). Therefore, we determined the effect of α1(AD) subunits on surface expression of α3 subunit-containing $GABA_ARs$.

We transfected HEK293T cells with 0.250 μg of α3, β2, and γ2 subunit cDNA and varying amounts (0–2 μg) of either α1 or α1(AD) subunits. As in the experiments in Fig. 4, we included the wild type α1 subunit to serve as a basis for comparison between α3 subunit substitution by the wild type α1 subunit and α1(AD)-mediated inhibition of expression. To emulate the $GABA_AR$ expression in ADJME patients who have two wild type *GABRA3* genes but only one wild type *GABRA1* gene, we transfected 0.250 μg of α3 subunit cDNA instead of 0.125 μg as we did for the hemizygous $\alpha1\beta2\gamma2$ conditions. We performed flow cytometry experiments and stained for surface α3 subunit expression.

Co-transfecting increasing amounts of α1(AD) subunit cDNA caused a concentration-dependent reduction in surface α3 subunit expression (Fig. 7, *A* and *B*). We confirmed the inhibition of α3 subunit expression using biotinylation assays and Western blots. We transfected cells with α3, β2, and γ2 subunits with or without 2 μg of α1(AD) subunit cDNA. We performed biotinylation assays and Western blots and found that α1(AD) subunits significantly reduced expression of surface α3 subunits (Fig. 7, *C* and *D*). As described in Fig. 4, we confirmed that the α1(AD) subunit did not inhibit $\alpha3\beta2\gamma2$ receptor expression by competing for transcriptional and translational machinery by measuring the effect of pmaxGFP on $\alpha3\beta2\gamma2$ receptor expression (supplemental Fig. 2*C*).

α1(AD) Subunits Reduced Surface Expression of α3 Subunit-containing $GABA_ARs$ to a Greater Extent than α1 Subunit-containing $GABA_ARs$—Surprisingly, when we compared the effects of α1(AD) subunits on surface expression of α1 (Fig. 4) and α3 (Fig. 7) subunits, we found that α1(AD) subunits reduced α3 subunit expression to a greater extent than α1 subunit expression (Fig. 8*A*). We next determined whether α1(AD) subunits also reduced surface expression of partnering β2 and $\gamma2^{HA}$ subunits to a greater extent when co-expressed with α3 subunits than with α1 subunits.

We co-transfected HEK293T cells with β2 and $\gamma2^{HA}$ subunits (0.250 μg), either hemizygous α1 (0.125 μg) or wild type α3 subunits, and a range (0–2 μg) of α1(AD) subunit cDNA. We measured surface $\gamma2^{HA}$ subunit expression by

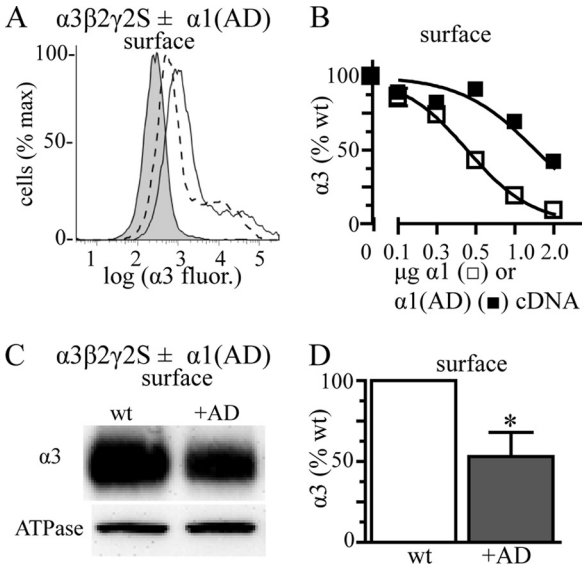

FIGURE 7. **Effect of the α1(AD) subunit on wild type α3β2γ2 $GABA_AR$.** We transfected HEK293T cells with empty vector (negative control, *shaded histogram*) or 0.250 μg of α3, β2, and γ2S subunits without any additional subunit (wild type) or with varying masses (0.125–2 μg) of mutant α1(AD) or wild type (*wt*) α1 subunit cDNA. We quantified the surface (*A* and *B*) α3 subunit expression using flow cytometry. *A*, we presented a sample flow cytometry histogram with wild type fluorescence as a *solid line* and wild type + 2 μg of α1(AD) fluorescence as a *dashed line*. *B*, we quantified the surface α3 subunit fluorescence in the presence of the different amounts of α1(AD) (■, $n \geq 4$) or wild type α1 (□, $n = 3$) subunit cDNA and normalized the α3 subunit fluorescence to that of wild type cells. Increasing the mass of α1(AD) and α1 subunit cDNA reduced surface α3 subunit expression. We also determined the effect of 2 μg of α1(AD) subunit cDNA co-transfection on surface α3β2γ2 receptor expression using biotinylation assays with Western blot (*C* and *D*). We stained the Western blots with the anti-α3 subunit antibody and quantified surface α3 subunit relative to that of the Na^+/K^+-ATPase α subunit (loading control). The presence of the α1(AD) subunit reduced surface expression of α3β2γ2 receptors by 47 ± 15% ($n = 6$; $p = 0.024$). *, $p < 0.05$.

flow cytometry and normalized the HA fluorescence to that obtained from hemizygous $\alpha1\beta2\gamma2^{HA}$ receptors (Fig. 8, *B* and *C*). This experiment demonstrated that in the absence of α1(AD) subunits, there was no significant difference in surface $\gamma2^{HA}$ subunit expression between $\alpha1\beta2\gamma2^{HA}$ and $\alpha3\beta2\gamma2^{HA}$ receptors (99 ± 5%). This result indicated that under these transfection conditions, cells express similar amounts of $\alpha1\beta2\gamma2^{HA}$ and $\alpha3\beta2\gamma2^{HA}$ receptors.

The addition of α1(AD) subunit reduced $\alpha3\beta2\gamma2^{HA}$ receptor expression to a greater extent than $\alpha1\beta2\gamma2^{HA}$ receptor expression. Interestingly, when cells expressing α1β2γ2 receptors were transfected with 0.250 and 0.500 μg of α1(A322D) subunits, there were small increases in $\gamma2^{HA}$ subunit expression, a result that may suggest that in a small fraction of receptors the α1(AD) subunit changes the composition of the $GABA_AR$ pentamer to one that contains more than one $\gamma2^{HA}$ subunit.

We performed biotinylation assays and Western blots as a second method to determine the effect of α1(AD) subunits on the surface expression of α3β2γ2 and α1β2γ2 receptors. We transfected HEK293T cells with α1β2γ2, α3β2γ2, $\alpha1\beta2\gamma2^{HA}$, or $\alpha3\beta2\gamma2^{HA}$ subunits and either with or without 2 μg of α1(AD) subunit cDNA. We performed biotinylation assays and Western blots to quantify the relative amounts of surface β2 and $\gamma2^{HA}$ subunits (Fig. 8, *D–G*). These experiments demonstrated that α1(AD) subunits reduced expression of surface β2 and $\gamma2^{HA}$ subunits to a greater extent when co-expressed with α3 subunits than with α1 subunits.

Unlike the transfected heterologous cells used in the previous experiments that expressed either α1 or α3 subunits, neurons simultaneously express an endogenous mixture of $GABA_AR$ subunits, including α1, α3, and other α subunit subtypes. Therefore, we next determined whether or not α1(AD) subunits would reduce surface expression of α3 subunits to a greater extent than α1 subunits in HEK293T cells simultaneously expressing both α1 and α3 subunit cDNA.

We transfected HEK293T cells with $\alpha1^h$, α3, β2, and $\gamma2^{HA}$ subunits (0.125:0.250:0.250:0.250 μg of cDNA ratio) and with or without 1 μg of $\alpha1(AD)^r$ subunit cDNA. We quantified the relative surface expression of $\alpha1^h$, α3, and $\gamma2^{HA}$ subunits using flow cytometry (Fig. 8, *H* and *I*). We found that $\alpha1(AD)^r$ subunits reduced expression of surface α3 subunits (30 ± 4%) to a greater extent than $\alpha1^h$ subunits (12 ± 4%, $p = 0.010$). $\alpha1(AD)^r$ subunits reduced expression of surface $\gamma2^{HA}$ subunits by a similar amount as it reduced surface $\alpha1^h$ subunit expression, 15 ± 1%. These results indicated that in cells expressing both α1 and α3 subunits, α1(AD) subunits produced a modest reduction in total surface $GABA_AR$ expression and conferred a greater reduction of $\alpha3\beta2\gamma2^{HA}$ than $\alpha1\beta2\gamma2^{HA}$ $GABA_ARs$. This would result in an alteration of the composition of surface $GABA_ARs$ to those with a greater fraction of α1 than α3 subunit-containing receptors.

AD Mutation Reduced α1(AD) Subunit Expression in Neurons—The previous experiments determined the effect of α1(AD) subunits on $GABA_ARs$ overexpressed in heterologous cells. Here, we determined the effect of α1(AD) subunits on endogenous $GABA_ARs$ in cultured neurons. To enable the non-destructive identification of transfected neurons without the use of large fluorescent fusion proteins, we inserted our cDNAs of interest into a commercial plasmid upstream of an internal ribosome entry site, which was followed by the cDNA encoding the fluorescent coral protein, ZsGreen1. We made five constructs by inserting either nothing (control), $\alpha1^h$, $\alpha1(AD)^h$, $\alpha1^{HA}$, or $\alpha1(AD)^{HA}$ subunits. Because these constructs expressed the cDNA of interest and the fluorescent protein as separate peptides, the fluorescent protein did not interfere with α1 subunit trafficking, post-translational modification, or function.

We obtained cortical neurons from E18 rats and established neuron-enriched cultures. We transfected neurons at DIV10 and analyzed them at DIV17, the time point at which the cultured neurons develop mature GABAergic synapses. We first characterized the composition of our neuronal cultures at DIV17. We measured the number of DAPI-positive nuclei that also stained with the neuron-specific marker NeuN. We found that 89 ± 5% of the cells were neurons ($n = 3$) and that the neuronal transfection efficiency was 4 ± 0.4% (data not shown). In these characterization experiments, no non-neuronal cells were transfected. However, in subsequent experiments, we did identify cells rarely with a non-neuronal morphology that expressed ZsGreen1; these non-neuronal cells were not included in the analyses.

We next determined the effect of the AD mutation on expression of α1(AD) subunits in neurons. We transfected

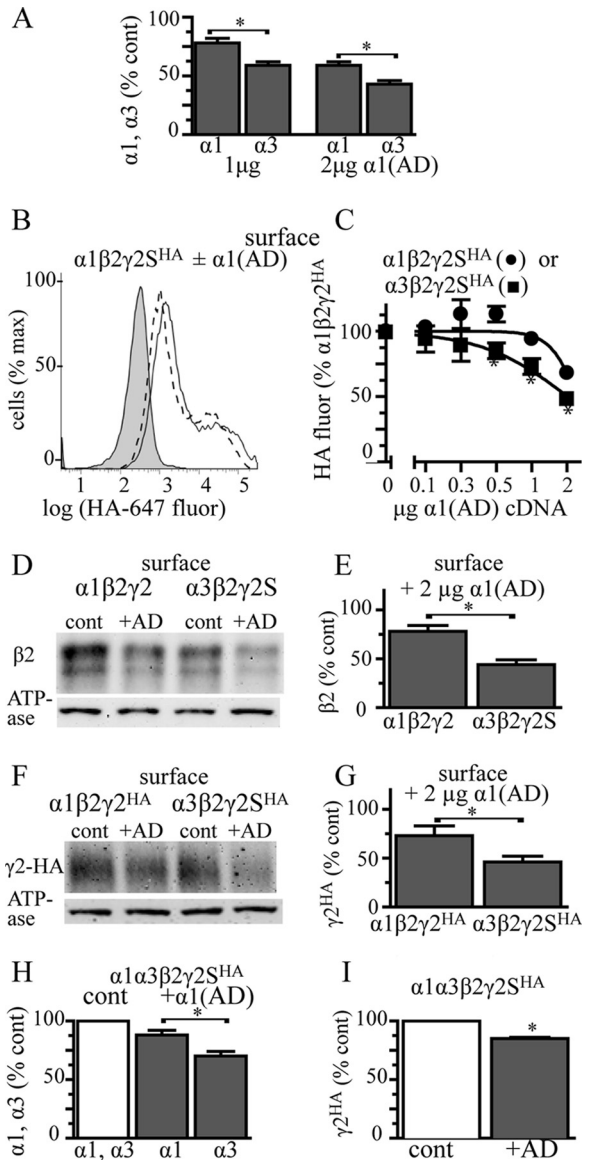

FIGURE 8. **Effect of the α1(AD) subunit on surface β2 and γ2 subunit expression in α1β2γ2 and α3β2γ2 receptors.** *A*, we replotted the data from Figs. 4 and 7 depicting the effect of 1.0 and 2.0 μg of $\alpha1(AD)^r$ subunit cDNA on surface α1 and α3 subunit expression. The $\alpha1(AD)^r$ subunit reduced surface α3 subunit expression to a greater extent than α1 subunit expression ($p < 0.002$). *B* and *C*, we transfected HEK293T cells with empty vector (negative control (*cont*)) or 0.250 μg of β2 and $\gamma2S^{HA}$ cDNA and either 0.125 μg of α1 subunit (hemizygous α1) or 0.250 α3 subunit (WT α3). We co-transfected different masses (0–2 μg) of mutant α1(AD) subunit cDNA. We quantified the surface $\gamma2S^{HA}$ subunit expression using an anti-HA antibody and flow cytometry. *B* presents a sample flow cytometry histogram that plots the $\gamma2^{HA}$ fluorescence *versus* the number of cells. Negative control fluorescence is *shaded*; fluorescence from $\alpha1\beta2\gamma2^{HA}$ receptors in the absence of the α1(AD) subunit is a *solid line,* and fluorescence from $\alpha1\beta2\gamma2^{HA}$ receptors + 2 μg of α1(AD) cDNA is a *dashed line*. *C*, we quantified the surface $\gamma2^{HA}$ expression for $\alpha1\beta2\gamma2^{HA}$ (●) and $\alpha3\beta2\gamma2^{HA}$ (■) receptors for each amount of α1(AD) subunit cDNA. The $\gamma2^{HA}$ subunit fluorescence was normalized to the $\gamma2^{HA}$ fluorescence in the $\alpha1\beta2\gamma2$ receptors in the absence of α1(AD) subunit. In the absence of the α1(AD) subunit, there was no significant difference in $\gamma2^{HA}$ expression between the $\alpha1\beta2\gamma2^{HA}$ and $\alpha3\beta2\gamma2^{HA}$ receptors (99 ± 5%, $p = 0.895$). Addition of the α1(AD) subunit caused concentration-dependent reductions in $\gamma2^{HA}$ subunit that were greater in $\alpha3\beta2\gamma2^{HA}$ than $\alpha1\beta2\gamma2^{HA}$ receptors (* $p < 0.05$, $n \geq 6$). Biotinylation and Western blot assays (*D–G*) demonstrated that transfecting 2 μg of α1(AD) subunit cDNA reduced surface β2 subunit expression to a greater extent in $\alpha3\beta2\gamma2$ receptors (56 ± 5%) than $\alpha1\beta2\gamma2$ receptors (22 ± 6%, $n = 5$, $p = 0.002$) and also reduced $\gamma2^{HA}$ subunit expression by a greater extent in $\alpha3\beta2\gamma2^{HA}$ receptors (54 ± 6%) than $\alpha1\beta2\gamma2^{HA}$ receptors (27 ± 10%, $n = 5$, $p = 0.049$). Finally, we transfected HEK293T cells with $\alpha1^h$, α3, β2, and $\gamma2^{HA}$ subunits in a 0.125:0.250:0.250:0.250 ratio and with or without 1.0 μg of $\alpha1(AD)^r$ subunit. We determined the amount of surface $\alpha1^h$, α3, and $\gamma2^{HA}$ subunit expression by flow cytometry. The $\alpha1(AD)^r$ subunit reduced α3 subunit expression (30 ± 4%) to a greater extent than $\alpha1^h$ subunit expression (12 ± 4%, $p = 0.010$, $n = 5$, *H*), and it reduced $\gamma2^{HA}$ expression by 15 ± 1% ($p = 0.001$, $n = 5$, *I*).

neurons with control-, $\alpha1^h$-, $\alpha1(AD)^h$-, $\alpha1^{HA}$-, or $\alpha1(AD)^{HA}$-IRES-ZsGreen1 constructs. We performed Western blots on neuronal lysates and stained them with either anti-$\alpha1^h$ or anti-HA antibodies. Visual inspection demonstrated that the AD mutation substantially reduced both $\alpha1(AD)^h$ and $\alpha1(AD)^{HA}$ subunit expression (Fig. 9, *A* and *B*). Because of weak signal, we could not quantify $\alpha1(AD)^h$ subunit expression on Western blot. Quantification of $\alpha1^{HA}$ and $\alpha1(AD)^{HA}$ subunit expression revealed that the AD mutation reduced $\alpha1(AD)^{HA}$ subunit expression by 39 ± 9%, a result consistent with what we and others reported for epitope-tagged α1(AD) subunits expressed in HEK293T cells (10, 11) and a much lower level of reduction than we typically observe using untagged α1 subunits (Fig. 1).

We used immunofluorescence studies to determine the effect of the mutation on untagged human $\alpha1(AD)^h$ subunit expression in neurons. We transfected neurons with control-, $\alpha1^h$-, or $\alpha1(AD)^h$-IRES-ZsGreen1 plasmids and analyzed total expression on DIV17. We fixed, permeabilized, and stained the neurons with anti-$\alpha1^h$ subunit antibody to quantify total recombinant $\alpha1^h$ and $\alpha1(AD)^h$ subunit expression. We identified transfected neurons by ZsGreen1 fluorescence (Fig. 9, *C* and *D*). Compared with wild type $\alpha1^h$ subunit-transfected neurons, there was no significant difference in ZsGreen1 fluorescence in control (103 ± 4%) or $\alpha1(AD)^h$ subunit (99 ± 12%)-transfected neurons.

The anti-$\alpha1^h$ antibody specifically labeled recombinant $\alpha1^h$ subunit protein. Neurons transfected with control vector ($n = 16$) possessed 2 ± 1% of the fluorescence of those transfected with $\alpha1^h$ subunits (data not shown). Both $\alpha1^h$ and $\alpha1(AD)^h$ subunits were expressed diffusely throughout the cytoplasm and dendrites and did not form any definite inclusions (Fig. 9, *E* and *F*). The intensity of ZsGreen1 fluorescence correlated with the intensity of both $\alpha1^h$ and $\alpha1(AD)^h$ subunit immunofluorescence (Fig. 9*G*). The AD mutation reduced $\alpha1(AD)^h$ subunit expression to 21 ± 9% that of the $\alpha1^h$ subunit (Fig. 9*H*).

Expression of the α1(AD) Subunits Altered Current Time Course and Reduced Peak Amplitude of mIPSCs—We determined whether expression of α1 and α1(AD) subunits altered mIPSC. We transfected neurons in five separate experiments with control-, α1-, or α1(AD)-IRES-ZsGreen1 constructs. On DIV17, we recorded more than 100 mIPSCs from pyramidally shaped ZsGreen1-positive neurons (Fig. 10*A*). We quantified the inter-mIPSC interval, rise time, decay time, and peak current amplitudes.

Transfection of wild type α1 subunits, but not α1(AD) subunits, caused a very small but statistically significant reduction in the inter-mIPSC interval compared with control transfection (median mIPSC interval reduced from 1.5 to 1.4 s, $p = 0.015$,

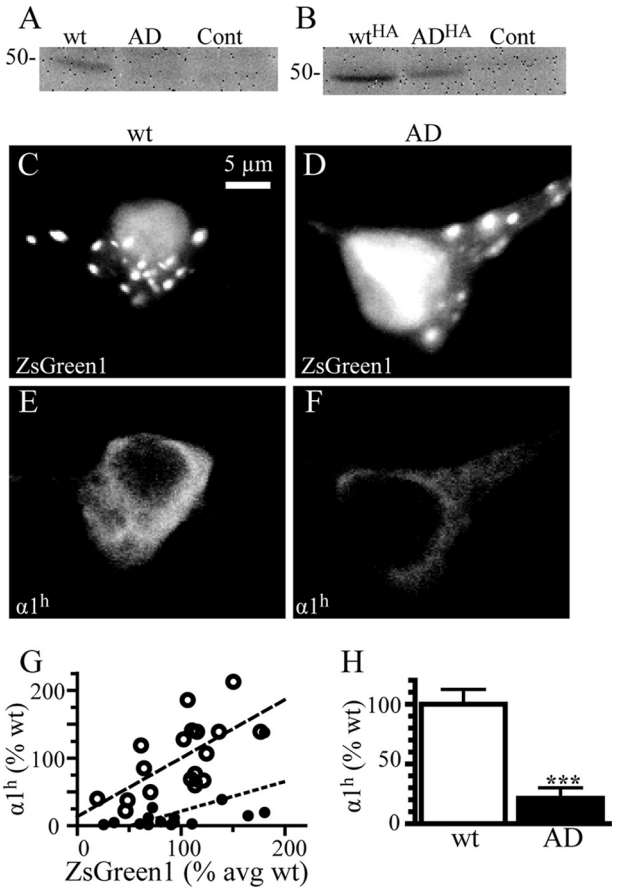

FIGURE 9. **Effect of the AD mutation on α1(AD) subunit expression in cultured cortical neurons.** We transfected DIV10 cultured cortical neurons with either control-IRES-ZsGreen1, $\alpha1^h$-IRES-ZsGreen1 (*wt*), $\alpha1(AD)^h$-IRES-ZsGreen1 (AD), $\alpha1^{HA}$-IRES-ZsGreen1 (WT^{HA}), or $\alpha1(AD)^{HA}$-IRES-ZsGreen1 (AD^{HA}). On DIV17, we performed Western blots of neuronal lysates and stained them with either the anti-$\alpha1^h$ antibody (*A*, $n = 4$) or the anti-HA antibody (*B*, $n = 5$). Visual inspection demonstrated that the mutation substantially reduced both $\alpha1(AD)^h$ and $\alpha1(AD)^{HA}$ expression. Because of weak signal intensity, the untagged human $\alpha1(AD)^h$ subunits in neuronal lysates could not be quantified. However, quantification of the gels stained with the anti-HA antibodies demonstrated that $\alpha1(AD)^{HA}$ subunit expression was reduced by 39 ± 9% compared with wild type $\alpha1^{HA}$ expression ($p = 0.010$). Next, in four separate experiments, we transfected DIV10 neurons with control-IRES-ZsGreen1, $\alpha1^h$-IRES-ZsGreen1 (*wt*), or $\alpha1(AD)^h$-IRES-ZsGreen1 (AD) and performed immunofluorescence studies on DIV17 to identify transfected neurons by ZsGreen1 fluorescence in the green channel (*C* and *D*) and recombinant $\alpha1^h$ and anti-$\alpha1(AD)^h$ subunit immunofluorescence in the red channel (*E* and *F*). Visual inspection demonstrated that the ZsGreen1 fluorescence localized primarily within the nuclei and in small puncta within the cytoplasm and that recombinant $\alpha1^h$ and $\alpha1(AD)^h$ subunits expressed diffusely throughout the soma and the dendrites. There was no significant difference in ZsGreen1 fluorescence among the control (103 ± 4%), $\alpha1^h$- (100 ± 9%) and $\alpha1(AD)^h$ (99 ± 12%)-transfected cells The anti-$\alpha1^h$ antibody specifically labeled recombinant $\alpha1^h$ protein with the neurons transfected with control vector ($n = 16$) having 2 ± 1% the A546 fluorescence as those transfected with $\alpha1^h$ (data not shown). The $\alpha1^h$ immunofluorescence intensity correlated with the ZsGreen1 intensity for both the samples transfected with $\alpha1^h$ (○, $p = 0.003$, $r^2 = 0.42$) and $\alpha1(AD)^h$ (●, $p = 0.017$, $r^2 = 0.35$) (*G*). Compared with neurons transfected with $\alpha1^h$ ($n = 18$), the neurons transfected with the $\alpha1(AD)^h$ subunit possessed 21 ± 9% of the $\alpha1^h$ immunoreactivity (*H*, $n = 16$, $p < 0.001$).

data not shown). The α1 and α1(AD) subunit conditions did not significantly differ from each other.

In contrast to the very modest effects of α1 subunit transfection on inter-mIPSC intervals, both α1 and α1(AD) subunits substantially altered mIPSC current kinetics, a result consistent with altered $GABA_AR$ composition. Compared with neurons transfected with control vector, neurons transfected with either α1 or α1(AD) subunits possessed reduced mIPSC rise (data not shown) and decay times (Fig. 10, *B* and *D*, $p < 0.001$). Moreover, transfection of the α1 subunit reduced mIPSC decay time to a greater extent than the α1(AD) subunit ($p < 0.001$). The change in the $GABA_AR$ mIPSC kinetics suggested a shift in receptor composition from non-α1 to α1 subunit-containing receptors, a change that could result if overexpressed wild type α1 subunits replaced non-α1 subunit-containing $GABA_ARs$ in synapses and if overexpressed mutant α1(AD) subunits prevented surface trafficking of non-α1 subunit-containing $GABA_ARs$ to a greater extent than α1 subunit-containing $GABA_ARs$. GABA-evoked currents from recombinant $GABA_ARs$ expressed in HEK293T cells revealed that of the four α subunit isoforms found in synaptic $GABA_ARs$ in the cerebrum (α1–3 and α5), only $GABA_ARs$ expressing the α3 subunits possessed slower deactivation rates than α1 subunit-containing $GABA_ARs$ (32). Therefore, it is likely that α1(AD) subunits selectively inhibited expression of α3 subunit-containing $GABA_ARs$.

In addition to altering mIPSC kinetics, the α1 and α1(AD) subunits also reduced mIPSC peak amplitudes (Fig. 10, *C* and *D*, $p < 0.001$). The effect of α1(AD) subunits on mIPSC peak amplitudes was consistent with its reduction of wild type $GABA_AR$ surface expression (Figs. 4, 7, and 8). The effect of α1 subunits on peak mIPSC amplitudes was unexpected because studies in heterologous cells demonstrated that $\alpha1\beta2\gamma2$ and $\alpha3\beta2\gamma2$ $GABA_ARs$ possess similar peak current amplitudes. Different possible mechanisms could explain this unexpected finding. First, the exact composition of endogenous synaptic $GABA_ARs$ is unknown. Although it is assumed that endogenous $GABA_ARs$ at DIV17 consist of a mixture of $\alpha1\beta2\gamma2$ and $\alpha3\beta2\gamma2$ receptors, it is possible that endogenous $GABA_ARs$ have a composition that demonstrates higher peak current amplitudes than the α1 subunit-containing $GABA_ARs$ that replace them. Second, it is also possible that overexpression of wild type α1 subunits could reduce mIPSC peak amplitudes by increasing the tonic, persistently active, currents of the neurons, which shunt synaptic currents (33). Although tonic currents are mediated by δ subunit-containing $GABA_ARs$ that typically co-assemble with either α4 or α6 subunits (34, 35), recent results demonstrated that they can also co-assemble with α1 subunits (36).

DISCUSSION

We and others reported that the AD mutation caused a loss of α1(AD) subunit expression and function (8, 10–13, 21, 26). Although the heterozygous loss of α1 subunits causes neuronal hyperexcitability, α1 subunit haploinsufficiency alone does not cause the full ADJME phenotype (14, 15, 28, 37). The main finding of this study is that residual, nondegraded α1(AD) subunits conferred a dominant effect that reduced $GABA_AR$ expression more than would result from haploinsufficiency alone. Unexpectedly, the α1(AD) subunit reduced expression of $\alpha3\beta2\gamma2$ receptors to a greater extent than $\alpha1\beta2\gamma2$ receptors. Although these effects were small, they likely contribute to the cortical excitability produced by the heterozygous reduction in

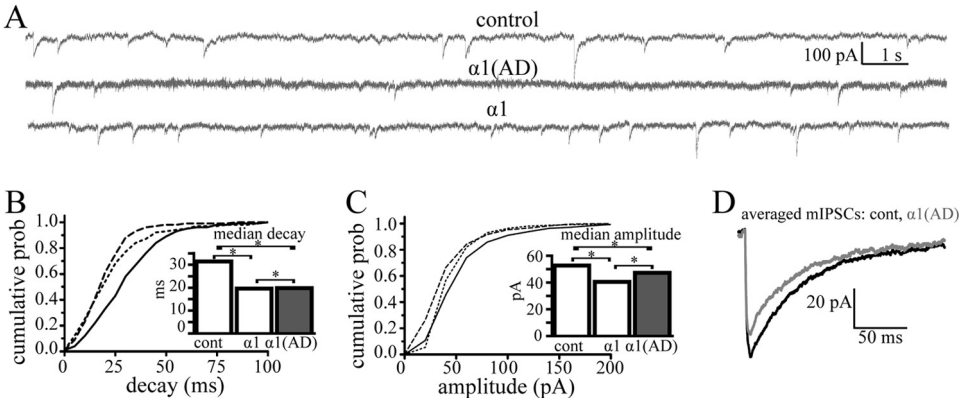

FIGURE 10. **Effect of the α1(AD) subunit on mIPSCs in cultured cortical neurons.** In five separate experiments, we transfected DIV10 cultured cortical neurons with either control-IRES-ZsGreen1 (control), α1-IRES-ZsGreen1 (wild type, α1), or α1(AD)-IRES-ZsGreen1 (α1(AD)). On DIV17, we identified transfected neurons by ZsGreen1 fluorescence and recorded >100 mIPSCs events from each. *A,* we showed sample mIPSC current traces. Transfection of both the α1 and α1(AD) subunit altered mIPSC current kinetics (*B* and *D*). *B,* we plotted a histogram that depicts the mIPSC decay time constants on the *abscissa* and the cumulative probability (*prob*) of an mIPSC having that decay time on the *ordinate*. Neurons transfected with control vector (*solid line*) had the biggest decay time constants followed by those transfected with α1(AD) (*dotted line*) and α1 (*dashed line*, $p < 0.001$). In the *inset*, we plotted the median mIPSC decay times. *C,* we plotted a histogram depicting mIPSC peak amplitudes on the *abscissa* and cumulative probability of a mIPSC having that peak amplitude on the *ordinate*. Neurons transfected with control subunit possessed larger mIPSC amplitudes than α1(AD)-transfected neurons, which possessed larger amplitudes than those transfected with α1 subunit ($p < 0.001$). The median mIPSC amplitudes are plotted in the *inset*. *D,* we displayed averaged (>100 events) mIPSC traces for wild type (*black*) and α1(AD)-transfected neurons (*gray*) demonstrating both the accelerated decay and reduced mIPSC amplitudes in neurons transfected with the α1(AD) subunit. *, $p < 0.05$.

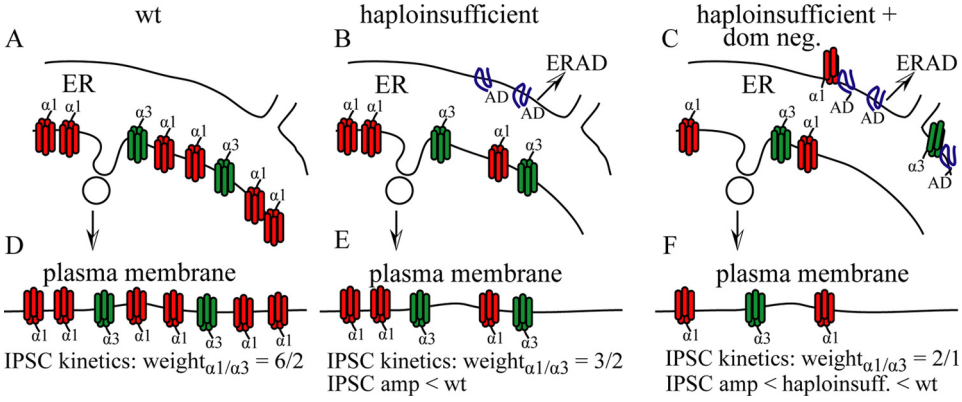

FIGURE 11. **Model of the effects of the α1(AD) subunit on surface $GABA_AR$ expression and isoform composition.** This figure depicts our model of how the α1(AD) subunit reduces wild type surface $GABA_AR$ expression and alters their composition. $GABA_ARs$ assemble in the ER (*A–C*) and traffic to the plasma membrane (*D--F*). At maturity, wild type neurons (*wt*, *A* and *D*) predominantly express α1β2γ2 receptors (*red*) but also express non-α1-containing $GABA_AR$ (depicted here as α3 $GABA_AR$, *green*), and thus we depicted a 6:2 ratio of α1β2γ2 to α3β2γ2 receptors. In a purely haploinsufficient model (*B* and *E*), all the misfolded α1(AD) subunit (*blue*) is degraded without it interacting with wild type $GABA_AR$. Therefore, haploinsufficient neurons express reduced α1β2γ2 receptors and unchanged non-α1-containing $GABA_AR$. The time course of the IPSC current kinetics would result from the currents contributed from α1 and α3 subunit containing receptors weighted by their abundance on the neuron surface. Therefore, as depicted here, the α1/α3 weighting would decrease from 6/2 in wild type neurons to 3/2 in α1 haploinsufficient neurons thus producing IPSCs that more resembled α3 subunit containing $GABA_AR$ in the haploinsufficient neurons compared with wild type neurons. Our data are more consistent with a haploinsufficient plus dominant negative model (*C* and *F*). In this model, neurons degrade some α1(AD) subunit but also retain some misfolded α1(AD) subunit (*blue*) in the ER, which can associate with and retain a greater fraction of α3β2γ2 than α1β2γ2 receptors. This is shown here as α1(AD) retaining 1/3 α1 subunit containing receptors and 1/2 α3 subunit containing receptors. The retention of wild type $GABA_AR$ expression in the haploinsufficient plus dominant negative case reduces IPSC peak amplitudes to a greater extent than in the α1 haploinsufficient neurons. In addition, the selective retention of α3 subunit containing receptors increases the α1/α3 weighting from 3/2 to 2/1 thus producing IPSC current kinetics that are more similar to α1 subunit containing $GABA_AR$ than in the α1 haploinsufficient condition.

functional α1 subunit expression and thus may shape the epilepsy phenotype.

α1(AD) Subunit Reduced α1β2γ2 Expression by Entrapping Wild Type $GABA_A$ Receptor Subunits within the ER—The disruption of wild type gene function by a mutant gene product can be accomplished by several mechanisms. A mutation may cause a nonspecific effect if it produces a toxic gene product that enhances cell death (25, 38) or represses protein synthesis through the unfolded protein response (39, 40). In addition, mutations in multimeric ion channels such as $GABA_ARs$ can cause specific effects by associating with wild type subunits and either forming dysfunctional ion channels on the cell surface, causing increased endocytosis, or preventing surface trafficking of the wild type protein complex.

Our study demonstrated that despite being grossly misfolded (10), the α1(AD) protein did not decrease HEK293T cell viability. In addition, overexpression of the α1(AD) subunit did not cause visible neuronal injury or death, alter neuronal physiology, or change neuronal membrane properties. In addition, the α1(AD) subunit did not nonspecifically reduce expression of transmembrane proteins unrelated to $GABA_ARs$ (Fig. 4). Our experiments also showed that even with substantial overexpression, the α1(AD) subunit did not produce a dominant negative effect by substituting for wild type $GABA_AR$ on the cell surface (Fig. 2) or increasing dynamin-mediated endocytosis of wild type α1β2γ2 receptors (Fig. 5).

The α1(AD) subunit did cause a dominant negative effect by producing specific, concentration-dependent reductions in expression of surface wild type $GABA_ARs$ (Figs. 4, 7, and 8). Because previous studies demonstrated that essentially all residual α1(AD) subunits were localized to the ER (21, 26), and because our experiments (Fig. 6) as well as those of Bradley *et al.* (11) showed that α1(AD) subunits specifically associated with wild type $GABA_AR$ subunits, we conclude that the α1(AD) subunit reduced expression of surface wild type $GABA_AR$ subunits by entrapping them within the ER. Moreover, our data provided direct evidence that the α1(AD) subunit reduced total as well as surface $GABA_AR$ expression (Fig. 4*B*), a result consistent with degradation of entrapped $GABA_AR$ subunits via ER-associated degradation (Fig. 11).

α1(AD) Subunit Reduced α3 Subunit Expression to a Greater Extent than α1 Subunit Expression—Homozygous *Gabra1* knock-out mice increase the protein expression of other α subunits, including the α3 subunit (28–30). Because increased synaptic expression of α3 subunits compensates for absent α1 subunits, we tested if α1(AD) subunits also reduced expression of α3 subunit-containing $GABA_A$Rs. Surprisingly, we found that α1(AD) subunits reduced the surface expression of α3β2γ2 receptors to a greater extent than α1β2γ2 receptors in HEK293T cells (Figs. 7 and 8). We also found that expression of α1(AD) subunits in cultured cortical neurons altered the time course of endogenous GABAergic mIPSCs, a result that suggested that non-α1 subunit-containing $GABA_A$Rs were replaced by α1 subunit-containing $GABA_A$Rs (Fig. 10). In ADJME patients, the extent to which α1(AD) subunits would preferentially inhibit expression of α3 subunit-containing receptors would depend on the amount of α1(AD) subunits expressed in endogenous conditions.

Different mechanisms could explain why α1(AD) subunits reduced α3β2γ2 receptors to a greater degree than α1β2γ2 receptors. A simple explanation would hold that α1(AD) subunits associate with α3 subunits with higher affinity than with α1 subunits and thus entrap a greater percentage of α3 subunits in the ER. Although functional $GABA_A$Rs that traffic to the cell surface require a defined subunit stoichiometry and assembly order *without* two adjacent α subunits (α-β-α-γ-β) (4–6, 41), it is possible that nonfunctional α1/α3 oligomers could form, be sequestered in the ER, and undergo ER-associated degradation.

α1(AD) subunits could also selectively reduce expression of surface α3β2γ2 receptors by sequestering β2 and γ2 subunits. If α1 and α1(AD) subunits have the same affinity for β2/γ2 subunits, and α3 subunits have a lower affinity for β2/γ2 subunits, the presence of α1(AD) subunits would deprive α3 subunits of their necessary assembly partners to a greater extent than α1 subunits. Previous studies identified domains within the extracellular region of α1 subunits that are responsible for its oligomerization with β2 and γ2 subunits (42–44). The β2 subunit binding domains in the α1 and α3 subunits are identical except for a single conserved substitution. However, the γ2 subunit binding domains have four differences, including nonconserved substitutions of a threonine to a lysine and an arginine to a proline. It would be of interest in future studies to determine whether γ2 subunits oligomerize with α3 subunits with lower affinity than with α1 subunits and if either of these two amino acids explains the difference.

Differences in oligomerization affinities between the α1 and α3 subunits with β2 or γ2 subunits would explain the differential effects of the α1(AD) subunit only if β2 or γ2 subunit expression was not in excess. However, our data in Fig. 3 demonstrated that at a fixed concentration of β2 and γ2 subunits, a 4-fold increase in α1 subunit cDNA produced corresponding increases in α1β2γ2 subunit expression, evidence that β2 and γ2 subunits were in excess. A mechanism that could explain a greater effect of α1(AD) subunits on α3β2γ2 receptors than α1β2γ2 receptors in conditions of excess β2 and γ2 subunits would be that α3β2γ2 receptors traffic to the cell surface at slower rates than α1β2γ2 receptors. In this case, α3β2γ2 receptors would be retained in the ER longer than α1β2γ2 receptors, which would provide them with more opportunity to incorporate an α1(AD) subunit and be targeted for degradation.

Although our experiments focused on determining the effect of α1(AD) subunits on α1β2γ2 and α3β2γ2 receptors, interactions of α1(AD) subunits with other $GABA_A$R subunits may make even more important contributions to the epilepsy phenotype. Future studies will be needed to determine the effects of α1(AD) subunits on expression of other $GABA_A$R isoforms.

Model of the Dominant Effect—We depicted our model for the effect of α1(AD) subunits on α1β2γ2 and α3β2γ2 receptors in Fig. 11. In this model, wild type neurons express both α1β2γ2 and α3β2γ2 receptors in the ER (Fig. 11*A*) and on the neuron surface (Fig. 11*D*). Because mature cortical neurons express more α1 than α3 subunits (1–3, 45), α1β2γ2 and α3β2γ2 receptors are shown here in a 6:2 ratio. The amplitude and time course of GABAergic currents would result from a weighted average of α1β2γ2 and α3β2γ2 currents. In a haploinsufficient model, the α1(AD) subunits are degraded and do not associate with wild type receptors. Therefore, in a completely haploinsufficient case, neurons express reduced α1β2γ2 receptors but the same amount of α3β2γ2 receptors in the ER (Fig. 11*B*) and the neuron surface (Fig. 11*E*). Therefore, in a haploinsufficient model, the reduction in α1β2γ2 but not α3β2γ2 expression would result in a greater proportion of α3β2γ2 receptors on the surface than found in wild type neurons (shown here as a 3:2 ratio). Therefore, the time course of GABAergic currents, as a weighted sum of the α1β2γ2 and α3β2γ2 receptors, would be more similar to that of α3β2γ2 receptors in haploinsufficient than wild type neurons. Because there would be fewer $GABA_A$R on the cell surface, inhibitory postsynaptic current peak amplitudes would be smaller in haploinsufficient than wild type neurons.

Rather than a haploinsufficient model, our data presented here suggests a haploinsufficient plus dominant negative model (Fig. 11, *C* and *F*). In this model, neurons express α1(AD) subunit in the ER. Some α1(AD) subunits degrade, but some α1(AD) subunits oligomerize with α1 and α3 subunit-containing $GABA_A$Rs (Fig. 11*C*). Retained α1(AD) subunits reduce a greater fraction of α3β2γ2 receptors than α1β2γ2 receptors, and thus the ratio of α1 to α3 subunit-containing receptors is shown here as a 2:1 ratio (Fig. 11*F*). The time course of the GABAergic currents is thus more similar to that of α1β2γ2 receptors in a haploinsufficient plus dominant negative model than in the pure haploinsufficient model. Because both α1β2γ2 and α3β2γ2 receptor expression is reduced, peak current amplitudes are reduced relative to wild type and haploinsufficient currents.

Implications of Dominant Negative Effects for ADJME and Other Dominant Epilepsy Syndromes—Although the amount of endogenous α1(AD) subunit expressed in neurons of ADJME patients is unknown, our data demonstrated that neurons degrade recombinant α1(AD) subunit with high efficiency (79%, Fig. 9). Therefore, assuming that the endogenous α1(AD) subunit in ADJME patients also expresses at 21% of wild type α1 subunit and that the α1(AD) subunit in neurons cause similar sigmoidal reductions in surface wild type α1 and α3 subunit expression as in HEK293T cells (Figs. 4, 7, and 8), we expect that heterozygous α1(AD) subunit expression in ADJME patients

would reduce surface α1 and α3 subunit expression by an additional 4 and 5%, respectively, more than hemizygous α1 subunit expression.

Could such a seemingly small additional reduction in surface α1 and α3 subunit expression alter the epilepsy phenotype? Both empirical and theoretical systems do suggest that seizures are threshold events and that even small changes in $GABA_AR$ availability can transition an organism into a seizure-prone state. For example, even though the $GABA_AR$ antagonists, bicuculline and pentylenetetrazole, inhibit GABA-evoked currents with typical sigmoidal concentration-response curves (46, 47), they produce seizures in experimental animals at specific doses with very small variances (48, 49). These findings suggest that a specific threshold of functional $GABA_ARs$ is required to prevent an organism from experiencing a seizure. Moreover, recent computational models of neural networks predicted that very small changes in ion channel function can produce seizure-like activities (50).

Small changes in $GABA_AR$ expression and composition may shape the phenotypes of other autosomal dominant $GABA_AR$ subunit mutations that are associated with epilepsy. The best studied mutation is the γ2(R43Q) mutation associated with childhood absence epilepsy and febrile seizures (51). The γ2(R43Q) subunit produces smaller changes in $GABA_AR$ expression and composition than the α1(AD) subunit. Although the R43Q mutation does not reduce the total expression of the γ2(R43Q) subunit, it disrupts its ability to directly oligomerize with β2 subunits (52). The inability of γ2(R43Q) subunits to oligomerize may explain why they do not produce a dominant negative effect on α1, α3, or β2 subunit expression or alter mIPSC amplitude or current kinetics (17, 18). The γ2(R43Q) subunit does reduce surface trafficking of the α5 subunit-containing $GABA_ARs$ and thereby reduces tonic $GABA_AR$ currents (17). Although the effects of the γ2(R43Q) subunit are small, they do shape the epilepsy phenotype because the heterozygous γ2(R43Q) subunit knock-in mice but not heterozygous γ2 subunit knock-out mice experience seizures (16, 19, 53).

Therefore, we think that the small dominant negative effects of the α1(AD) subunit could confer an epilepsy phenotype that is different from the one conferred by α1 subunit haploinsufficiency alone. This hypothesis needs to be directly tested by comparing heterozygous α1 knock-out with α1(AD) knock-in genetically modified mice.

Acknowledgments—We thank Dr. Bruce Carter (Vanderbilt University) for helpful comments concerning this manuscript. Flow cytometry experiments were performed in the VMC Flow Cytometry Shared Resource. The Vanderbilt University Medical Center Flow Cytometry Shared Resource is supported by the Vanderbilt Ingram Cancer Center Grant P30 CA68485 and the Vanderbilt Digestive Disease Research Center Grant DK058404. Flow cytometry was supported in part by National Institutes of Health Vanderbilt CTSA Grant 5UL1 RR024975-03 from NCRR.

REFERENCES

1. Brooks-Kayal, A. R., Jin, H., Price, M., and Dichter, M. A. (1998) *J. Neurochem.* **70,** 1017–1028
2. Laurie, D. J., Wisden, W., and Seeburg, P. H. (1992) *J. Neurosci.* **12,** 4151–4172
3. Pirker, S., Schwarzer, C., Wieselthaler, A., Sieghart, W., and Sperk, G. (2000) *Neuroscience* **101,** 815–850
4. Tretter, V., Ehya, N., Fuchs, K., and Sieghart, W. (1997) *J. Neurosci.* **17,** 2728–2737
5. Baumann, S. W., Baur, R., and Sigel, E. (2001) *J. Biol. Chem.* **276,** 36275–36280
6. Baumann, S. W., Baur, R., and Sigel, E. (2002) *J. Biol. Chem.* **277,** 46020–46025
7. Macdonald, R. L., Kang, J. Q., and Gallagher, M. J. (2010) *J. Physiol.* **588,** 1861–1869
8. Cossette, P., Liu, L., Brisebois, K., Dong, H., Lortie, A., Vanasse, M., Saint-Hilaire, J. M., Carmant, L., Verner, A., Lu, W. Y., Wang, Y. T., and Rouleau, G. A. (2002) *Nat. Genet.* **31,** 184–189
9. Alfradique, I., and Vasconcelos, M. M. (2007) *Arq Neuropsiquiatr.* **65,** 1266–1271
10. Gallagher, M. J., Ding, L., Maheshwari, A., and Macdonald, R. L. (2007) *Proc. Natl. Acad. Sci. U.S.A.* **104,** 12999–13004
11. Bradley, C. A., Taghibiglou, C., Collingridge, G. L., and Wang, Y. T. (2008) *J. Biol. Chem.* **283,** 22043–22050
12. Fisher, J. L. (2004) *Neuropharmacology* **46,** 629–637
13. Gallagher, M. J., Song, L., Arain, F., and Macdonald, R. L. (2004) *J. Neurosci.* **24,** 5570–5578
14. Kang, J. Q., Shen, W., and Macdonald, R. L. (2009) *J. Neurosci.* **29,** 2833–2844
15. Maljevic, S., Krampfl, K., Cobilanschi, J., Tilgen, N., Beyer, S., Weber, Y. G., Schlesinger, F., Ursu, D., Melzer, W., Cossette, P., Bufler, J., Lerche, H., and Heils, A. (2006) *Ann. Neurol.* **59,** 983–987
16. Berry, R. B., Chandra, D., Diaz-Granados, J. L., Homanics, G. E., and Matthews, D. B. (2009) *Neurosci. Lett.* **455,** 84–87
17. Eugène, E., Depienne, C., Baulac, S., Baulac, M., Fritschy, J. M., Le Guern, E., Miles, R., and Poncer, J. C. (2007) *J. Neurosci.* **27,** 14108–14116
18. Frugier, G., Coussen, F., Giraud, M. F., Odessa, M. F., Emerit, M. B., Boué-Grabot, E., and Garret, M. (2007) *J. Biol. Chem.* **282,** 3819–3828
19. Tan, H. O., Reid, C. A., Single, F. N., Davies, P. J., Chiu, C., Murphy, S., Clarke, A. L., Dibbens, L., Krestel, H., Mulley, J. C., Jones, M. V., Seeburg, P. H., Sakmann, B., Berkovic, S. F., Sprengel, R., and Petrou, S. (2007) *Proc. Natl. Acad. Sci. U.S.A.* **104,** 17536–17541
20. Zeiger, S. L., Musiek, E. S., Zanoni, G., Vidari, G., Morrow, J. D., Milne, G. J., and McLaughlin, B. (2009) *Free Radic. Biol. Med.* **47,** 1422–1431
21. Gallagher, M. J., Shen, W., Song, L., and Macdonald, R. L. (2005) *J. Biol. Chem.* **280,** 37995–38004
22. Jiang, M., and Chen, G. (2006) *Nat. Protoc.* **1,** 695–700
23. Saliba, R. S., Pangalos, M., and Moss, S. J. (2008) *J. Biol. Chem.* **283,** 18538–18544
24. Lo, W. Y., Botzolakis, E. J., Tang, X., and Macdonald, R. L. (2008) *J. Biol. Chem.* **283,** 29740–29752
25. Zhao, J., Matthies, D. S., Botzolakis, E. J., Macdonald, R. L., Blakely, R. D., and Hedera, P. (2008) *J. Neurosci.* **28,** 13938–13951
26. Krampfl, K., Maljevic, S., Cossette, P., Ziegler, E., Rouleau, G. A., Lerche, H., and Bufler, J. (2005) *Eur. J. Neurosci.* **22,** 10–20
27. Kumar, A., Kremer, K. N., Sims, O. L., and Hedin, K. E. (2009) *Methods Enzymol.* **460,** 379–397
28. Kralic, J. E., Korpi, E. R., O'Buckley, T. K., Homanics, G. E., and Morrow, A. L. (2002) *J. Pharmacol. Exp. Ther.* **302,** 1037–1045
29. Kralic, J. E., Sidler, C., Parpan, F., Homanics, G. E., Morrow, A. L., and Fritschy, J. M. (2006) *J. Comp. Neurol.* **495,** 408–421
30. Ogris, W., Lehner, R., Fuchs, K., Furtmüller, B., Höger, H., Homanics, G. E., and Sieghart, W. (2006) *J. Neurochem.* **96,** 136–147
31. Bosman, L. W., Heinen, K., Spijker, S., and Brussaard, A. B. (2005) *J. Neurophysiol.* **94,** 338–346
32. Picton, A. J., and Fisher, J. L. (2007) *Brain Res.* **1165,** 40–49
33. Brickley, S. G., Cull-Candy, S. G., and Farrant, M. (1996) *J. Physiol.* **497,** 753–759
34. Jones, A., Korpi, E. R., McKernan, R. M., Pelz, R., Nusser, Z., Mäkelä, R., Mellor, J. R., Pollard, S., Bahn, S., Stephenson, F. A., Randall, A. D., Sieghart, W., Somogyi, P., Smith, A. J., and Wisden, W. (1997) *J. Neurosci.*

17, 1350–1362
35. Sur, C., Farrar, S. J., Kerby, J., Whiting, P. J., Atack, J. R., and McKernan, R. M. (1999) *Mol. Pharmacol.* **56,** 110–115
36. Glykys, J., Peng, Z., Chandra, D., Homanics, G. E., Houser, C. R., and Mody, I. (2007) *Nat. Neurosci.* **10,** 40–48
37. Kralic, J. E., O'Buckley, T. K., Khisti, R. T., Hodge, C. W., Homanics, G. E., and Morrow, A. L. (2002) *Neuropharmacology* **43,** 685–694
38. Szegezdi, E., Logue, S. E., Gorman, A. M., and Samali, A. (2006) *EMBO Rep.* **7,** 880–885
39. Page, K. M., Heblich, F., Davies, A., Butcher, A. J., Leroy, J., Bertaso, F., Pratt, W. S., and Dolphin, A. C. (2004) *J. Neurosci.* **24,** 5400–5409
40. Page, K. M., Heblich, F., Margas, W., Pratt, W. S., Nieto-Rostro, M., Chaggar, K., Sandhu, K., Davies, A., and Dolphin, A. C. (2010) *J. Biol. Chem.* **285,** 835–844
41. Connolly, C. N., Krishek, B. J., McDonald, B. J., Smart, T. G., and Moss, S. J. (1996) *J. Biol. Chem.* **271,** 89–96
42. Klausberger, T., Sarto, I., Ehya, N., Fuchs, K., Furtmuller, R., Mayer, B., Huck, S., and Sieghart, W. (2001) *J. Neurosci* **21,** 9124–9133
43. Bollan, K., King, D., Robertson, L. A., Brown, K., Taylor, P. M., Moss, S. J., and Connolly, C. N. (2003) *J. Biol. Chem.* **278,** 4747–4755
44. Bollan, K., Robertson, L. A., Tang, H., and Connolly, C. N. (2003) *Biochem. Soc. Trans.* **31,** 875–879
45. Poulter, M. O., Barker, J. L., O'Carroll, A. M., Lolait, S. J., and Mahan, L. C. (1992) *J. Neurosci.* **12,** 2888–2900
46. Zhang, J., Xue, F., and Chang, Y. (2008) *Mol. Pharmacol.* **74,** 941–951
47. Huang, R. Q., Bell-Horner, C. L., Dibas, M. I., Covey, D. F., Drewe, J. A., and Dillon, G. H. (2001) *J. Pharmacol. Exp. Ther.* **298,** 986–995
48. Vlainiæ, J., and Periciæ, D. (2009) *Neuropharmacology* **56,** 1124–1130
49. Hentschke, M., Wiemann, M., Hentschke, S., Kurth, I., Hermans-Borgmeyer, I., Seidenbecher, T., Jentsch, T. J., Gal, A., and Hübner, C. A. (2006) *Mol. Cell. Biol.* **26,** 182–191
50. Thomas, E. A., Reid, C. A., Berkovic, S. F., and Petrou, S. (2009) *Arch. Neurol.* **66,** 1225–1232
51. Wallace, R. H., Marini, C., Petrou, S., Harkin, L. A., Bowser, D. N., Panchal, R. G., Williams, D. A., Sutherland, G. R., Mulley, J. C., Scheffer, I. E., and Berkovic, S. F. (2001) *Nat. Genet.* **28,** 49–52
52. Hales, T. G., Tang, H., Bollan, K. A., Johnson, S. J., King, D. P., McDonald, N. A., Cheng, A., and Connolly, C. N. (2005) *Mol. Cell. Neurosci.* **29,** 120–127
53. Chiu, C., Reid, C. A., Tan, H. O., Davies, P. J., Single, F. N., Koukoulas, I., Berkovic, S. F., Tan, S. S., Sprengel, R., Jones, M. V., and Petrou, S. (2008) *Ann. Neurol.* **64,** 284–293